Treball de Fi de Grau

Enginyeria en Tecnologies Industrials

Modelling of an energy storage system using redox flow batteries

MEMÒRIA

Autor: Albert Alcalde Bru

Director: Ramon Costa Castelló

Convocatòria: Juliol 2019

Escola Tècnica Superior
d'Enginyeria Industrial de Barcelona

ABSTRACT

In the context of the world's transition to more environmentally friendly activities, energy plays a big role. The replacement of fossil fuels for renewable energies will be pivotal in the following years but it will not be an easy process.

Redox flow batteries and, specifically, vanadium redox flow batteries can be a helping hand in that path. They are unique energy-storing technologies that could complement and solve some of the current drawbacks of renewable energies.

The aim of this project is to, first, understand the general principles behind the redox flow batteries. The second goal is to develop a working model of a vanadium redox flow battery based on existing mathematical equations that describe their behaviour. The third and final objective is to design a control system for the battery so that it could automatically and reliably deliver a desired voltage set arbitrarily (within its capabilities).

To achieve the goals of the project, a first analysis of redox flow batteries is conducted, including the search for the equations that will be able to govern the dynamic system. With these equations and to be able to linearize the system, equilibrium points will be found and analysed. With a linear system and while working close to its equilibrium points, it will be possible to design a controller that can ensure the functioning of the battery at a certain voltage. After this process, some simulations will be run to observe the behaviour of the system that has been built, placing emphasis on factors such as its reliability or its capacity to work under different conditions.

To finish off, conclusions will be drawn from all the previous work, research and results, bearing in mind that the field of redox flow batteries is still at its early stages.

SUMMARY

1. PREFACE

1.1. Motivation

Every activity in the world shares one common trait: it is powered by energy. Changes of tides, pressure differences that result in wind, heat from inside the earth, even ATP in the case of living beings, and the list goes on.

This project combines this interesting and extensive topic with more technical fields. Starting with the biggest part of it, control engineering. With industry 4.0 in full swing, the automation and control of processes keeps extending. The work behind it is not easy and requires a combination of knowledge of maths and programming.

Another science that takes place in this project is chemistry, a lot of the energy processes that happen in the world are explained by chemistry, and the one tackled in this project is no different. Physics are involved as well, but they could even be used further if there was interest to dive deeper in some of the topics that will be treated, for example, the fluid mechanics in the pumping of the flow.

On a personal level, I enjoy all these disciplines, and I like the opportunity to learn more things related with programming and working with MATLAB and Simulink, as well as becoming more comfortable with them and improving what I have learnt throughout my bachelor's degree. Renewable energies and energy storing systems have always interested me.

What has motivated me to take on this project is the mixture of disciplines and the general interest of this subject, the possibility of learning new things from different points of view, and the chance to improve in some areas that I am already more familiar with.

1.2. Objective

The focus of this project will be put in the modelling of a vanadium redox flow battery system with the help of MATLAB and Simulink, taking into account things such as the chemistry in the battery cells, the physics of the electricity that charge and discharge the battery, the dimensions of its components, etc.

With this model, some experiments will be carried out in order to see how the variables interact with each other and to better understand the behaviour of these type of systems.

A control system will be designed to automatically control the battery so it can store or deliver a certain electric current at a set voltage. The particular objective of the battery of the project is to work at the scale of a family home, where it can store unused energy from solar panels, for example, and deliver energy when the sun goes down or it gets cloudy.

Another part of the objective, not as technical as the others and more to do with research of the topic, is to know current the situation of these type of batteries, its place in the rise of renewable energies and get a peek on how possible future applications could pan out.

2. INTRODUCTION

2.1. Current energy situation

In this day and age of climate change in which taking care of the environment has become such a pivotal topic in society a lot of industries are working towards transforming everything from the ground up to make it more sustainable.

One of the most important and influential factors to try and readdress the climatic situation is the use of renewable energies. As seen in Figure 1, some countries have almost managed to fully produce their electricity only using renewable sources; for example, Iceland, Costa Rica and Sweden. Iceland in particular is leading the charge by quite a margin; it generates the cleanest electricity per person on earth, with about 85% of its energy coming from renewable sources [1]. Costa Rica is able to meet a large part of its energy needs from hydroelectric, geothermal, solar and wind sources; what is more, it has managed to run on just renewable energies for more than 300 days [2].

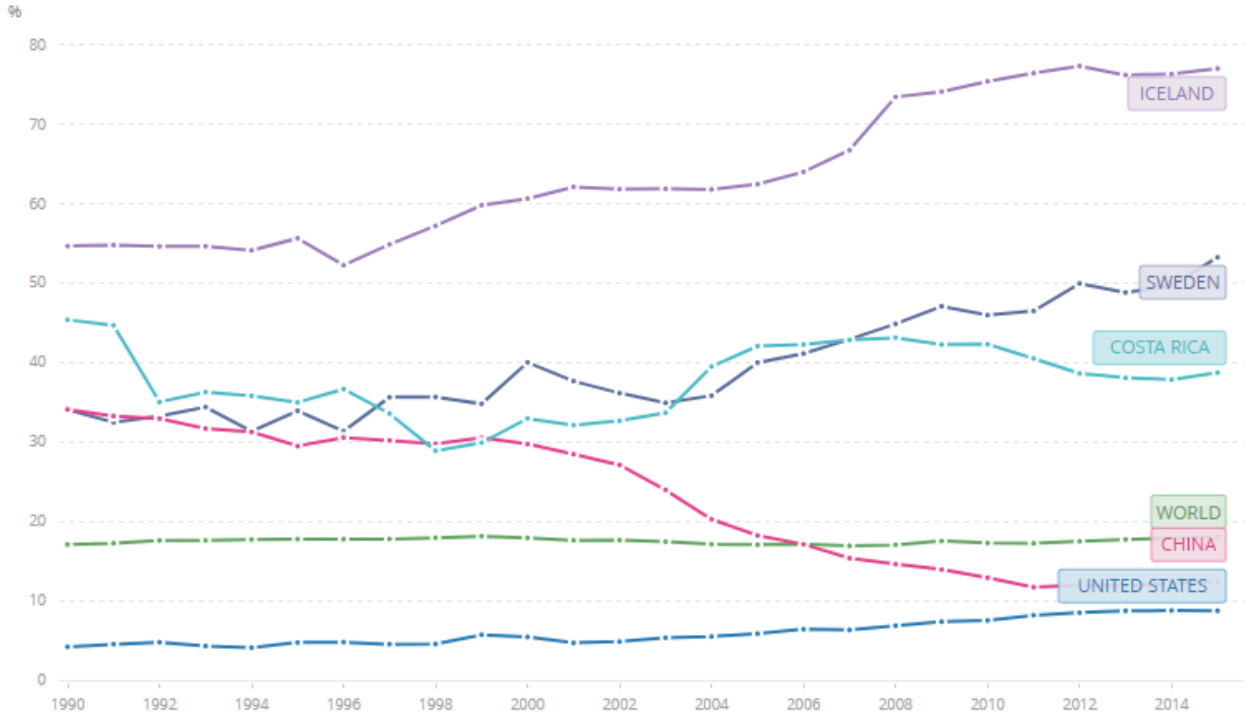

Figure 1. Renewable energy consumption (source: data.worldbank.org). The left axis shows the % of renewable energy consumed compared to the total consumption.

Some of the main economic and industrial powerhouses are the ones that need to catch up the most as it seems clear in Figure x. Perhaps it is a bit unfair to compare all regions in the world with these two specific countries, since their unique landscape allows for an easier harvest of energy, Costa Rica has 67 volcanoes and an all-year-long sunny climate, and Iceland heavily relies on geothermal energy both for electricity production and house heating. For this reason, Sweden can be a better role-model for the rest of the countries, since its progress is mainly due to the economic effort of the country to invest in solar power, wind power and smart grids amongst other technologies; still, hydropower and bioenergy remain the top renewable sources of energy in Sweden [3].

A recurrent problem when countries try to commit to using renewable energies is the impossibility to control the sources of energy. The sun is not always shining, wind is not always blowing, rivers do not always run full, etc. For example, the Netherlands is a country that, despite being in the forefront of many aspects of society, is heavily lagging behind when it comes to the use of renewable energies. The geography in the country is not ideal, the flat and mostly sub-sea level landscape limit the potential of hydropower resources, but on the flipside, winds are quite frequent and strong and in this aspect, the Netherlands is one of Europe's leading countries considering its size [4], nevertheless, wind is an uncontrollable and somewhat unpredictable source of energy. The Netherlands is not the only country that faces the problem of not being able to rely on many sources of renewable power; these types of regions will need to invest a lot of money on research and development in order to prevent this dependency on just one system of producing energy. This seems like the most plausible and realistic solution, unless the technology allows to store this excess energy. Some products that hint towards this are already in the market, albeit in a much lower scale and at a high price point; this is the case, for instance, of the so-called power walls which are stationary batteries, such as the one in Figure 2, intended to be used for home energy storage of electricity produced by solar panels [5].

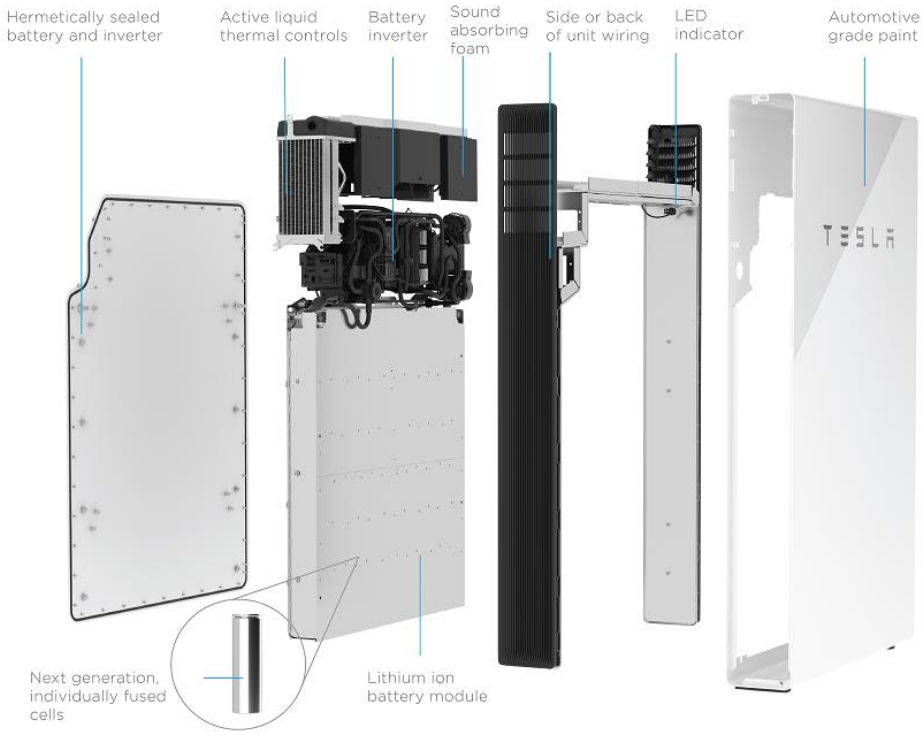

Figure 2. Tesla Powerwall [6].

Another example of the need to cut on fossil fuels is the renaissance of the electric car (Figure 3). All of the world's most important car manufacturers are releasing and/or planning to release new versions of their models that fully function with electric power. This progress seems to go at a high pace, but there are still some drawbacks that make people sceptical of making the change. Some of them are not true can be easily debunked, such as the argument that the emissions made to generate the electricity that powers the vehicle are the same that the emissions of a car with a combustion engine, which is untrue even if you generate this electricity by the most carbon intensive energy [7]. Perhaps the biggest one is the inconvenience of needing quite a lot more time to charge when compared to just needing to fill a tank with fuel. Companies like Tesla are putting a lot of effort into engineering ways to make the process as fast as possible [8], but maybe the level of convenience of regular fuel powered cars will never be matched with the current style of batteries in electric cars.

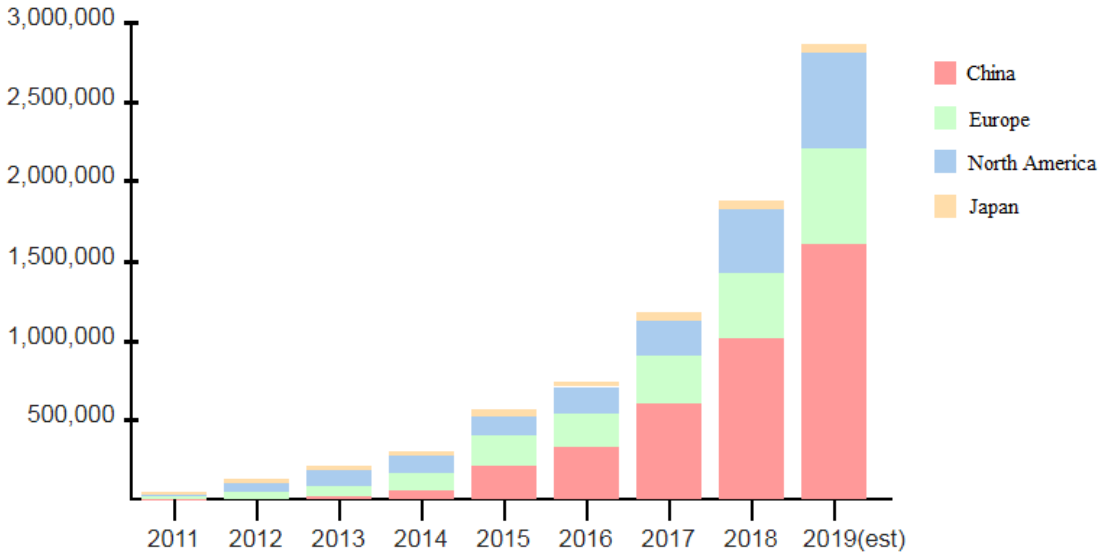

Figure 3. Annual sales of light-duty electric vehicles in the world's top markets [9].

One possible solution that could somehow mitigate some of the problems being mentioned would be to store energy whenever there is an excess of it. This is easier said than done, since the logistics for this are very complicated. To begin with, batteries can only be charged or discharged at certain rates; the Joule effect is the responsible for this, the bigger the current that circulates through an electrical system is, the greater the heat that it generates. Conventional batteries are prone to overheating, and high temperatures are very detrimental for them since they are the main responsible for their degradation overtime; this degradation, of course, keeps on reducing the maximum amount of energy that the battery was capable of storing when it was brand new.

2.2. Batteries

2.2.1. Redox reaction

Batteries are devices that store chemical energy in the form of more negatively charged ions and their more positively charged counterparts. These ions, that are isolated from each other normally, would cause a redox reaction if they were mixed together. A redox reaction is a chemical reaction that happens between two species, in which one of the species gains electrons while the other one loses them. This event results in both of the species changing their oxidation state: the species that gives the electrons to the other is called the reducer or

reducing agent, and the one that takes them is called the oxidizer or oxidizing agent. Applying this definition to the ions stored in a battery, the ion with the lower state of oxidation (more negatively charged) is the reducer, and the ion with the higher state of oxidation (more positively charged) is the oxidizer, a schematic can be seen in Figure 4 (where A and B represent a couple of chemical species that undergo a redox reaction).

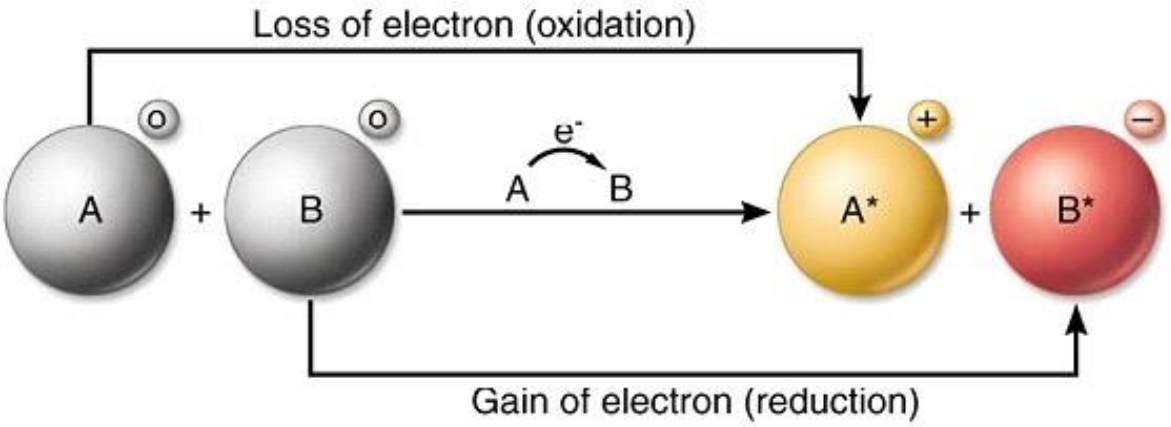

Figure 4. Redox reaction [10].

In order to make this reaction happen, the isolation between the two species of the battery needs to be broken. Since redox reactions are mainly based on an exchange of electrons, the two ions don't need to be in direct contact. Thanks to this, batteries can be used to provide electric energy to circuits, connecting the two poles of a battery with an electric conductor creates a pathway between the reducer and the oxidizer to exchange their electrons; if this electric circuit contains elements that work by consuming electric power between the positive and the negative pole, the flow of electrons will provide that necessary power to make them function.

What is interesting about some types of batteries is that the same process can be reversed, or in other words, the redox reaction can go both ways. Conventional use of batteries takes advantage of the energy derived from a certain redox reaction, however, the same reaction that provides energy can, sometimes, be reversed if it receives energy. Thanks to this phenomenon, rechargeable batteries exist. A schematic of a battery used both providing and storing energy can be seen in Figure 5.

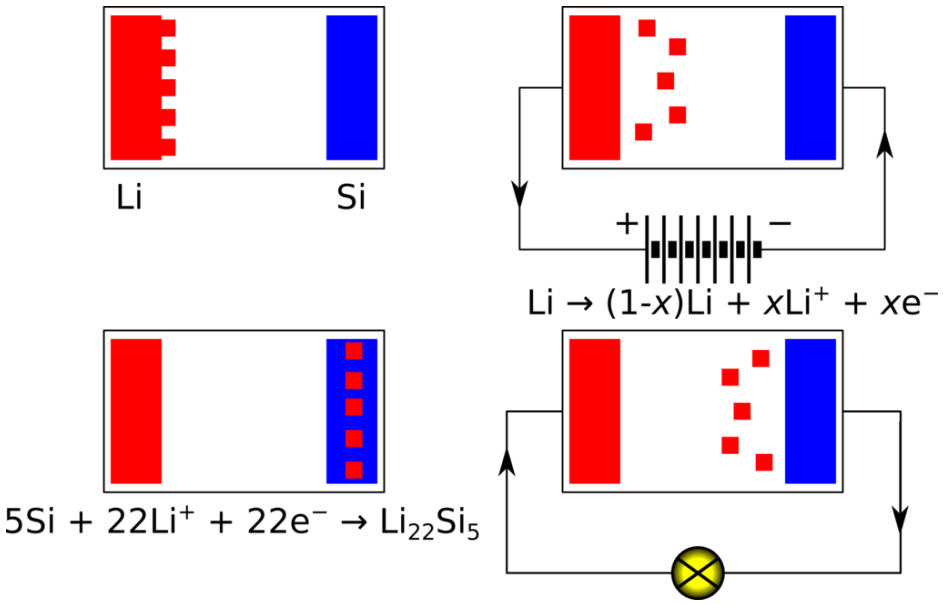

Figure 5. Scheme of a lithium-ion battery and its redox reaction [11].

Rechargeable batteries can be charged, discharged into an electrical load and recharged again a lot of times. Nevertheless, conventional batteries, and specifically lithium-ion batteries -which are the most commercially successful type of rechargeable battery-, lose their maximum energy storing capacity over time, even when they are not mistreated whatsoever; this is known as battery degradation. Battery degradation happens even when the battery is resting (not giving nor receiving energy), however, -as previously mentioned- high temperatures and putting the battery through multiple cycles of charging and discharging are the main causes of battery degradation and can really reduce their lifetime [12].

2.2.2. Types of batteries

Electric batteries have existed for two centuries now. There are two main families of batteries, both mentioned already: primary or disposable batteries (the ones that cannot be recharged), and secondary or rechargeable batteries (the ones that can indeed be recharged). This second group can be further classified into different types of batteries based on their chemistry, for instance [13], [14]:

- **Nickel-cadmium batteries:**

The nickel-cadmium battery main strengths are the maintenance of its cell voltage and the conservation of their charge when not in use. This type of batteries have a good life cycle and perform well at low temperatures. Some of their most usual applications are found in

portable electronic devices, toys; in a bigger scale, they are also used as aircraft starting batteries and in some electric vehicles.

- **Nickel-metal hydride batteries:**

The nickel-metal hydride battery shares one of its ions with the nickel-cadmium battery, Nickel. The other ion, however, is a hydrogen-absorbing alloy. The applications for this type of battery are mainly in high drain devices due to their high energy density and capacity.

- **Lead-acid batteries:**

Lead-acid batteries' main advantage is their low cost and reliability for heavy duty applications. They are big and heavy and are usually used for applications that allow for a non-portable source of power. This type of batteries were the first rechargeable ones, but they are still in use nowadays; their attributes and low cost makes them useful for high current applications like backup power supplies or starting automobile motors. The main disadvantage of lead is that it's extremely toxic: long-term exposure to tiny amounts of lead can cause damage to the brain, kidney and auditory system.

- **Lithium-ion batteries:**

Lithium-ion batteries, as mentioned previously, are one of the most extensively used kind of rechargeable batteries. They are found, for example, in smartphones and smart devices or, in the larger scale, in electric cars and military applications due to their lightweight nature.

Figure 6. Lithium-ion battery [14].

Depending on which ion is paired with the lithium, these batteries can slightly differ in their properties. In handheld devices, cobalt is usually the ion that accompanies lithium; it gives high energy density and low safety risks when damaged because of an accidental fall or similar factors. In the medical field and for powering electric tools, the lithium is paired with iron phosphate, which offers a lower energy density.

2.2.3. Redox flow battery

The main difference between redox flow batteries (RFBs) and the ones mentioned in the section before is that the anode and the cathode of the cell, the two parts that separate the reactants of a battery, are found in two separate tanks. Electroactive components are dissolved in the electrolyte in these tanks [15]. The majority of RFBs use two redox couples as the ions used to gain or deliver energy, with each couple stored in each tank.

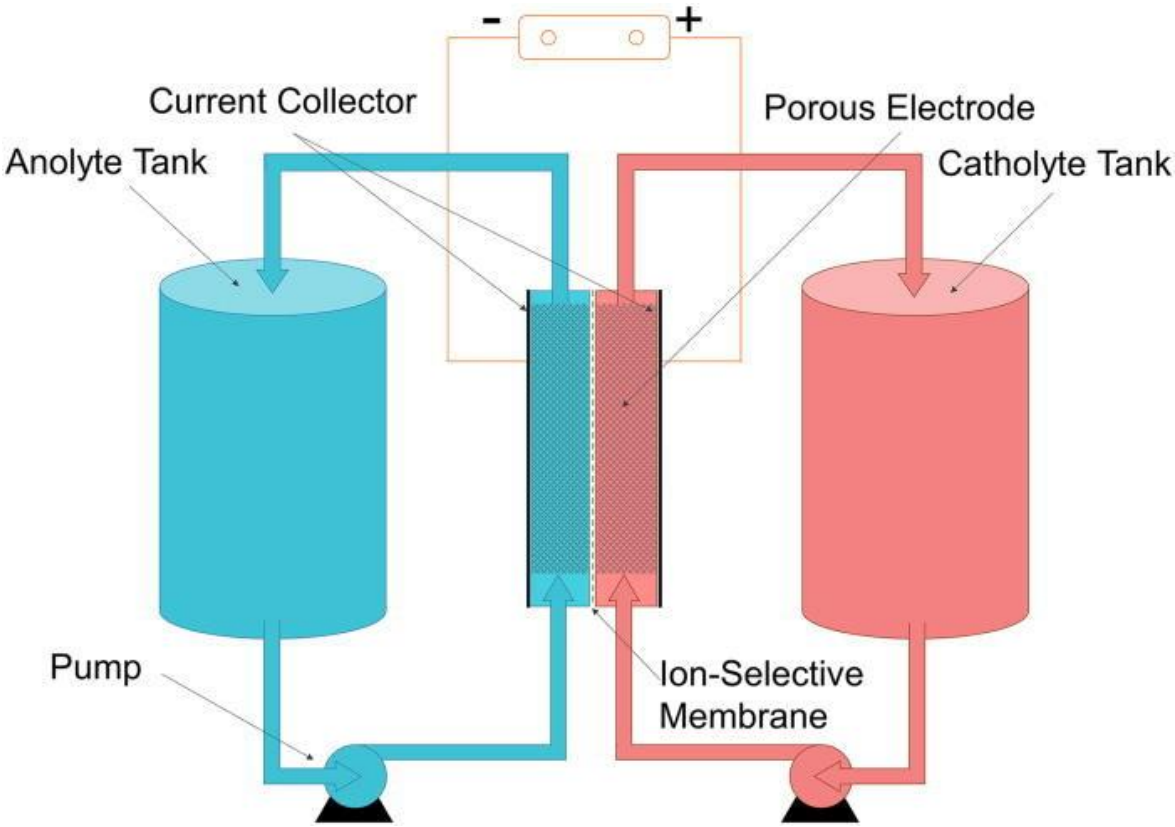

Figure 7. Redox flow battery schematic [16].

As seen in Figure 7, the redox flow battery is formed by flow cells (electrodes), which act as a meeting point for the ions. The fluids of the tanks are pumped in two closed loops through the battery stacks (which consist of a number of flow cells stacked together) and do the redox reaction inside the battery stack through an ion-exchange membrane. The new species after the reaction are then recirculated back to the tank thanks to the closed loop.

This way of functioning implies that the energy is stored in the two tanks. There are several advantages, such as the ability to design two tanks according to what each application of these batteries requires. Traditional rechargeable batteries do not have this ability.

Some of the potential applications of RFBs range from load levelling and peak shaving, uninterruptible power supplies for important electronic systems, emergency backups in health-related infrastructures.

More attractions for the rechargeable RFB systems in contrast to other types of conventional electrochemical batteries are: the simplicity of their electrode reactions, the ability to operate in low temperatures, a long cycle life for the redox couples, the possibility of reversible reactions (that is why they can be rechargeable), relatively few issues when the system becomes fully discharged, a quite clean and environmentally healthy manufacturing, use and disposal (without presence of heavy metals in all three stages).

One of the most important assets of RFBs is that the energy capacity and the power of the systems can be separated. The energy storage capacity depends on the concentration and volume of electrolytes in the tank while the power of the system depends on the number of cells in the stack and the size of the electrodes [17].

Of course, not everything that RFBs have to offer are advantages. One of the main drawbacks which have to be targeted and improved are the self-discharge shunt currents, which are low-resistance paths that let the current go around a certain point in the circuit and therefore losing some of the power contained in that current. When building the batteries, these paths need to be considered and be treated so as to increase their resistance; this can be done by increasing the ionic resistance of the flow ports, making the length of collector longer or reducing the cross-section of the ports [18].

A second disadvantage is the low energy density of RFBs, these provokes that the size of the needed tanks that can store or deliver a useful amount of energy need to be quite large. To add to that, the charge and discharge rates are low when compared to other means of energy storage; and to increase them, the electrodes and the membranes of the battery also need to be large. These two factors make the cost of RFBs not as cheap as the majority of other energy storage technologies.

Another disadvantage of RFBs when compared to more traditional batteries is their lack of efficiency. A lot of the body of work in the field of redox flow batteries aims to keep improving the methods that can lead to a higher efficiency of the technology [19].

2.2.4. Vanadium redox flow battery

Vanadium redox flow batteries (VRFB) are still in their early stages of life. The feasibility of VRFB was proved in the 1980s [20]. VRFBs are a particular type of redox flow batteries that takes advantage of the four different oxidation states of vanadium; this gives VRFBs a benefit that other RFBs don't have: no cross contamination by diffusion of ions since they are working with just one electroactive element dissolved in water.

The chemical reaction that happens in the negative cell of a VRFB battery is the following [17]:

$$V^{3+} + e^{-} \rightarrow V^{2+}$$

And in the positive cell:

$$VO^{2+} + H_2O \leftrightarrow VO_2^{+} + 2H^{+} + e^{-}$$

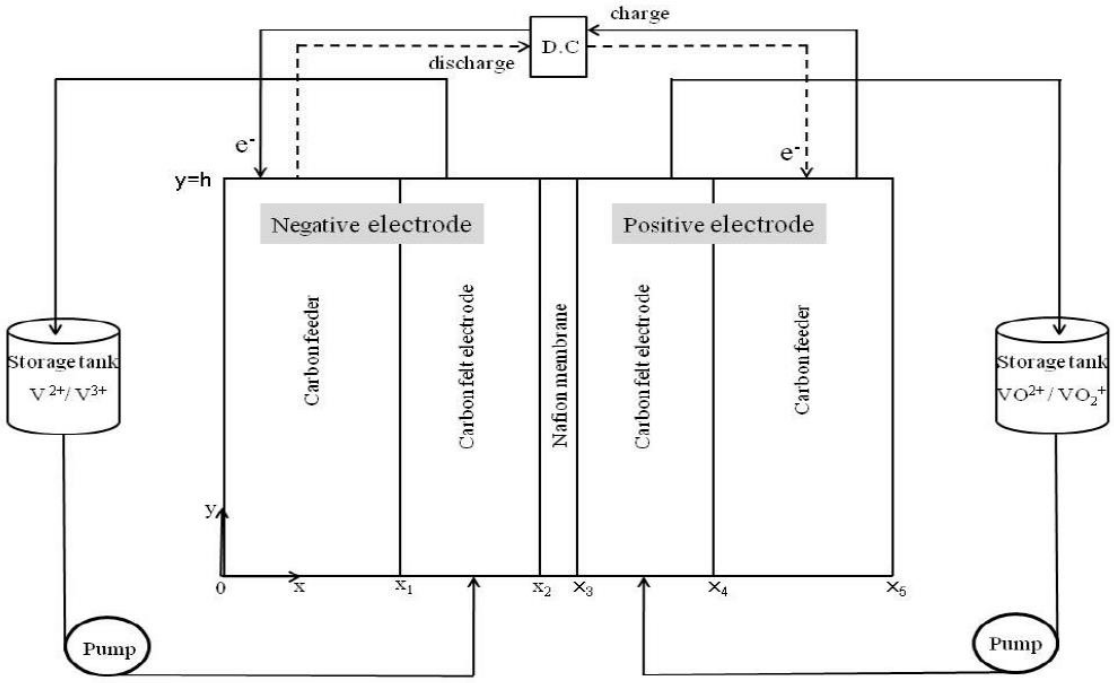

Figure 8. Schematic of a vanadium redox flow battery [17].

VRFBs, as it usually happens with redox flow batteries, have a rather low energy density (25 Wh/kg) if compared to more commercially dominant batteries such as the lead-acid (30-

40 Wh/kg) or the lithium-ion (80-200 Wh/kg). Some methods are being tested to improve this density like the use of precipitation inhibitors or the control of the ions' temperature.

Vanadium redox flow batteries have many advantages to compensate for this drawback nonetheless [21]:

- The chemical solutions have a long life, meaning that only the mechanical components of the system need replacement at the end of their life.
- As tackled before in the RFB battery description, instant recharge is possible by replacing the solutions. This makes it an attractive option for the, also previously mentioned problem, of electric vehicles and their lack of recharging convenience when compared to the usual combustion engines.
- The battery capacity can be increased by making the volume of solution larger.
- The vanadium battery has few detrimental effects when fully discharged.
- The cost per kWh decreases as the capacity increases. Large scale applications are benefited by this relation.
- Monitoring the whole capacity of the system can be easily done by monitoring the state of charge of the electrolytes as vanadium's colour depends on its oxidation state: V(II) is purple, V(III) is green, V(IV) is blue and V(V) is yellow (Figure 9).
- As with the majority of RFBs, the vanadium battery is environmentally friendly because it doesn't produce any waste products.
- Thanks to the low toxicity of the components, VRFBs could potentially be used in households that are powered by irregular renewable energies such as solar power. Getting charged when the energy produced is not used and supplying energy at night or in a cloudy day.

Figure 9. Vanadium colours based on their oxidation state [22].

3. EQUATIONS AND SYSTEM PARAMETERS

3.1. Cell concentrations

The chemical model used for the simulations is based on the differential equations that most commonly appear in the existing body of work of VRB storage systems. These differential equations take the concentrations of the vanadium species as a function of the current that goes through the cell and the flow rate of the dissolution [21].

These assumptions are made in order to get to the following equations are [23]:

- Temperature is constant.
- Oxygen and hydrogen evolution from water are neglected.
- No mass transfer across the membrane is considered.
- Perfect mixture is obtained in tanks and cells.
- All cells of a stack are equally well supplied with electrolyte.
- Concentration of VO_2^+ ions in the positive and of V^{2+} ions in the negative half-cell is always bigger than zero.
- Side-reactions caused by diffusion of vanadium ions across the membrane are instantaneous. This means that there exist no V^{2+} and V^{3+} ions in the positive half-cell and no VO_2^+ and VO^{2+} ions in the negative half-cell.
- The current vector represents a charging process. Changing its sign will represent a discharging process.

$$V_{HC}\frac{d}{dt}\begin{pmatrix} c_{2,c} \\ c_{3,c} \\ c_{4,c} \\ c_{5,c} \end{pmatrix} = \frac{1}{F}\begin{pmatrix} I \\ -I \\ -I \\ I \end{pmatrix} + Q_{HC}\begin{pmatrix} c_{2,t} & c_{2,c} \\ c_{3,t} & c_{3,c} \\ c_{4,t} & c_{4,c} \\ c_{5,t} & c_{5,c} \end{pmatrix} + \frac{A_C}{d_M}\begin{pmatrix} -D_2 & 0 & -D_4 & -2D_5 \\ 0 & -D_3 & 2D_4 & 3D_5 \\ 3D_2 & 2D_3 & -D_4 & 0 \\ -2D_2 & -D_3 & 0 & -D_5 \end{pmatrix} \cdot \begin{pmatrix} c_{2,c} \\ c_{3,c} \\ c_{4,c} \\ c_{5,c} \end{pmatrix} \quad (1)$$

The variables and constants that appear in (1) can be seen in Table 1.

Table 1. Variables and constants.

V_{HC}	Half-cell volume	[m^3]	**Subscript *i***	**Species**
$c_{i,c}$	Cell output concentration	[mol/m^3]	**2**	V^{2+}
F	Faraday constant	96485 [C/mol]	**3**	V^{3+}
I	Average cell current	[A]	**4**	VO^{2+}
Q_{HC}	Half-cell flowrate	[m^3/s]	**5**	VO_2^+
$c_{i,t}$	Tank concentration	[mol/m^3]		
A_C	Cell active area	[m^2]		
d_M	Membrane thickness	[m]		
D_i	Diffusion coefficient	[m^2/s]		

It is important to notice in (1) that the part of the equation that considers the diffusivity of vanadium with the diffusion coefficients also depends on the active area on which the dissolution will go through, and the length of thickness of that membrane. The diffusion coefficients of any chemical species are different for any specific pair of species and they are also dependant on the temperature and the porosity of the diffusion medium. In this project, the influence of temperature will not be considered thoroughly.

The variables associated with the diffusions in the cell, specifically, the cell active area $A_{C,}$ and the membrane thickness d_M that affect the rate of diffusion of the species mentioned in the paragraph before. Since all these constant values have to be set, both the diffusion coefficients D_i and the dimensions of the cell will be the same as in reference [23] which is inspired on a concrete type of ion exchanging membrane, the Nafion 115 membrane.

To make things simple, it will be assumed that both tanks (the anode and the cathode) are always equally charged, that means that concentrations of V^{2+} ions and VO_2^+ ions will be equal at all times; the same thing will happen with concentrations of V^{3+} ions and VO^{2+}ions. This simplification opens a new manner of taking tank concentrations into account, which will allow for an easier way to see how these concentrations affect the charging and

discharging of the battery, particularly when it comes to the currents and flow rates in these processes. This will be tackled later on.

Tank concentrations will be now set through the *SOC* (state of charge) and the total vanadium concentration of the tank c_v in the following way [24]:

$$SOC = \frac{c_{2,t}}{c_{2,t} + c_{3,t}} = \frac{c_{5,t}}{c_{4,t} + c_{5,t}} = \frac{c_{2,t}}{c_v} = \frac{c_{5,t}}{c_v} \tag{2}$$

Thus,

$$c_{2,t} = c_{5,t} = c_v \cdot SOC$$

$$c_{3,t} = c_{4,t} = c_v \cdot (1 - SOC)$$

It is important to bear in mind that SOC can take values from 0 to 1; however, in upcoming equations, the values of these two extremes will result in divisions by 0, therefore, all the simulations and graphic plotting will be done with SOC ranging from 0.1 to 0.9 (10% to 90%).

With this, the parameters for (1) that will be set at a constant value all throughout the project are the following:

Table 2. Constant parameters.

$\boldsymbol{A_C}$	0.02 [m^2]	$\boldsymbol{D}_2$	$4.4380 \cdot 10^{-12}$ [m^2/s]
$\boldsymbol{d_M}$	$1.27 \cdot 10^{-4}$ [m]	$\boldsymbol{D}_3$	$1.0024 \cdot 10^{-12}$ [m^2/s]
$\boldsymbol{c_v}$	$2 \cdot 10^3$ [mol/m^3]	$\boldsymbol{D}_4$	$3.8000 \cdot 10^{-12}$ [m^2/s]
		$\boldsymbol{D}_5$	$1.7500 \cdot 10^{-12}$ [m^2/s]

3.2. Tank concentrations

For the purpose of simplifying the model, it will be assumed that the rate at which the tank concentrations vary is so tiny that the effect it has on the cell concentration model is negligible. Even though the concentrations will not be considered for that, it is interesting to add a little appendix to the Simulink model that can show how these tiny variations in

concentrations happen throughout the simulations. The justification behind this decision is that the size of VRFBs' tanks is usually very big in comparison to the sizes of the cells.

To do this appendix, the following differential equations will be modelled:

$$V_{tank}\frac{d}{dt}\begin{pmatrix} c_{2,t} \\ c_{3,t} \\ c_{4,t} \\ c_{5,t} \end{pmatrix} = n \cdot Q_{cell}\left[\begin{pmatrix} c_{2,c} \\ c_{3,c} \\ c_{4,c} \\ c_{5,c} \end{pmatrix} - \begin{pmatrix} c_{2,t} \\ c_{3,t} \\ c_{4,t} \\ c_{5,t} \end{pmatrix}\right] \quad (3)$$

V_{tank} is the volume of the tank, Q_{cell} is now the flowrate of the whole cell and n is the number of cells in the stack.

3.3. Cell voltage

Cell voltage is an important parameter for this project: it is a very easily measurable magnitude directly related to the power consumption or generation of an electrical system. This relationship is completed with the current of said electrical system ($P = V \cdot I$).

In the case of VRFB, the cell voltage is given by the following equation, found in references [23], [24] and [25]:

$$E_{cell} = E_{formal} + \frac{RT}{F}\ln\left(\frac{c_{2,c} \cdot c_{5,c}}{c_{3,c} \cdot c_{4,c}}\right) \quad (4)$$

where E_{formal} is the formal potential of a cell and considered to be 1.4 V, T is the temperature -which will be considered constant at 298 K in all the calculations-, R is the universal gas constant with a value of 8.31 J/(mol·K) and F is the Faraday constant.

Of course, with a stack of n cells, the voltage will become $n \cdot E_{cell}$.

3.4. Battery sizing

Before diving deep into modelling these equations and reproducing the behaviour they symbolize, some variables are yet to be set. Specifically, the tank volume V_{tank}, the half-cell volume V_{HC}, and the number of connected cells in the stack n. To do so, it is important to remember that the purpose of this battery system is to serve the needs of an average home.

- **Tank sizing:**

Starting off with the tank volume, it will be sized so it can store at least a month's worth of ordinary power consumption. This way, it can sustain a house in continually adverse energy situations, such as the autumns in northern countries where daylight can be as brief as 4 hours a day and solar power struggles in this season, but it is still used as it thrives in spring and summer. Plus, sizing it this way will make sure that the tank size is big enough so that the assumption that the tank concentrations change very slowly can be true.

As mentioned in section 2.2.4, the specific energy of VRFBs usually stands at about 25 Wh/kg. As for density, the vanadium dissolution is done in water; the total vanadium concentration point that will be used, 2 mol/L, and with the atomic mass of vanadium being 50.94 atomic mass units, an estimated density of about 1100 kg/m^3 can be a good estimation.

As a reference for energy consumption, a 4 people house in Barcelona with modern and efficient home appliances including power hungry devices such as an AC, furnace, electric heating and even an electric car consumes an average monthly energy of 340 kWh [26].

Considering that in the colder months the consumption can go up (400 kWh will be assumed) and running some simple calculations:

$$V_{tank} = 3.4 \cdot 10^5\ Wh \cdot \frac{kg}{25\ Wh} \cdot \frac{m^3}{1100\ kg} = 12.36\ m^3$$

- **Cell stack sizing:**

As hinted before, taking a glance at equation (4) one can see that the model will have problems at either when either $c_{3,c}$, $c_{4,c}$ or both are really tiny, since the argument inside of the logarithm will tend to infinity; and it will also be an issue if either $c_{2,c}$, $c_{5,c}$ or both are really tiny, because then the argument inside of the logarithm will tend to 0. For that reason, the cell concentration values in the Simulink model will be limited at a value of 0.5% of the total vanadium concentration c_v, this means that they will not be able to go lower than 10 mol/m^3.

Also, since there is no cross contamination through the ion exchange membrane and the volume of the whole solution of each tank does not change, the maximum value of concentration for a certain electrolyte can never be bigger than c_v.

The above considerations guarantee that the voltage will not skyrocket to unreasonable values. In the current body of work, the maximum achievable values of voltage of a single

VRFB cell oscillates between 1.6 V [28] and 1.7 V [27], [23] (for future calculations 1.65 V will be picked as the maximum voltage, which is an average of the two values previously mentioned). It is convenient to remember that the formal circuit voltage of the cell is 1.4 V, which means that one single cell cannot play with a lot of margin (about 0.25 V) if the voltage that it delivers is to be controlled. For this particular reason, cell stacks are used when working with VRFBs in order to increase the overall voltage of the system and the ability to have a bigger margin to play with. This project will be no different.

To determine the number of connected cells in the stack, the example of the home in Barcelona will be used again: the tool that was used to determine the weekly energy consumption also suggested that the optimal hired power would be of 6.5 kW.

The currents that are usually worked with in the body of work of VRFB systems range between 20 to 150 A. The best efficiency in VRFBs is achieved at lower currents but, of course, working at lower current implies that the battery stack has to deliver more voltage to result in the same power, which results in putting more cells in the stack. With this in mind, it seems reasonable to assume that the normal conditions of work of the battery should be values in between the two mentioned extremes. As an example, the research on battery efficiency in reference [23] is checked at currents between 60 A and 100 A both for charging and discharging.

All in all, a value of 100 A will be used as the current at which the battery is capable of delivering the hired power of 6.5 kW, thus maintaining a reasonably good efficiency at that power while the same time not needing an unnecessarily large number of cells in the cell stack.

With this, the maximum voltage for the cell stack to be able to deliver the hired power at 100 A will be:

$$E_{stack} = \frac{P}{I} = \frac{6500\ W}{100\ A} = 65\ V$$

Thus, the number of cells in the stack to achieve this voltage, considering a maximum voltage per cell of 1.65 V, will have to be:

$$n = \frac{E_{stack}}{E_{cell}} = \frac{65}{1.65} = 39.4 \rightarrow 40 \text{ cells}$$

It is important to note that when the battery has to deliver power, it will need to be connected to some equipment, so it can deliver at similar conditions as the electric network.

When it comes to the volume of half a cell, the work in reference [29] is quite useful, as it contains a table that relates the delivered power with the cell active area. The closest values to the ones in the table are with a cell active area of 0.25 m^2 (a little more than in this model) and 5 kW (a little less than in this model); this yields a total stack volume of 0.49 m^3, operating and bearing in mind that the interest is on half a cell:

$$V_{HC} = \frac{1}{2} \cdot \frac{V_{stack}}{n} = \frac{1}{2} \cdot \frac{0.49}{40} = 0.0061\ m^3$$

4. THE MODEL

4.1. Equilibrium points

The equilibrium point of a system is a constant solution to the differential equation that governs it. To find an equilibrium point, the time derivative of the differential equation needs to be equal to zero. This implies that at that point, the system does not change throughout time, making it stationary instead of transient. The mathematical points that allow this to happen configure a so-called steady state [30].

Finding the equilibrium points can be done in various ways. MATLAB offers various functions which take all the user given parameters and returns the equilibrium point for it, *trim()* is an example of a function that does exactly that. With it, one of the ways to find multiple equilibrium points of a system is to build an iteration that keeps on changing the system parameters and stores the resulting equilibrium points for all of them. A better alternative which allows for more information and ease of use is to find the actual equation that yields the equilibrium point. Of course, for very complex systems this cannot always be possible, but for the case of this project, the equations are "simple" enough that they can be solved algebraically.

The matrix equation first presented in the previous section is the one that will be solved in order to find the equations for the equilibrium points of the concentrations.

$$\frac{d}{dt}\begin{pmatrix} c_{2,c}^{out} \\ c_{3,c}^{out} \\ c_{4,c}^{out} \\ c_{5,c}^{out} \end{pmatrix} = 0; \qquad \text{and therefore:}$$

$$0 = \frac{1}{F}\begin{pmatrix} I \\ -I \\ -I \\ I \end{pmatrix} + Q_{HC}\begin{pmatrix} c_{2,t} & c_{2,c} \\ c_{3,t} & c_{3,c} \\ c_{4,t} - & c_{4,c} \\ c_{5,t} & c_{5,c} \end{pmatrix} + \frac{A_C}{d_M}\begin{pmatrix} -D_2 & 0 & -D_4 & -2D_5 \\ 0 & -D_3 & 2D_4 & 3D_5 \\ 3D_2 & 2D_3 & -D_4 & 0 \\ -2D_2 & -D_3 & 0 & -D_5 \end{pmatrix} \times \begin{pmatrix} c_{2,c} \\ c_{3,c} \\ c_{4,c} \\ c_{5,c} \end{pmatrix} \tag{5}$$

Since one of the purposes of this project is to design a controller that works with the average cell currents I and the half-cell flowrate Q_{HC}, the equation is solved as a function of these two variables.

Solving (5) is done algebraically via the MATLAB equations and systems symbolic solver. Doing it algebraically opens up different possibilities that would be more tedious if the equilibrium points were found numerically and with iterations. One example of this convenience is that it will be easier and more efficient (it will require less computing time and resources) to see how the equilibrium concentrations behave at certain currents and flowrates, making it easier to plot the relationships between them.

Now that the equations for the equilibrium points are available, it is interesting to see how the concentrations for each species at each equilibrium point vary. For this, an iteration will be done in MATLAB (code available in annex) in which various flowrates and various average currents will result in different concentrations. In other words, the value for the concentrations, the current and the flowrate will result in a 3D point that will turn into a 3D surface with the iterations.

Currents will be iterated from 10 to 150 A in steps of 1 A. Flowrates will be iterated from $2 \cdot 10^{-6}$ to $5 \cdot 10^{-5}$ m^3/s in steps of $5 \cdot 10^{-7}$ m^3/s. As a reminder, the concentrations of the equilibrium points are the cell concentrations.

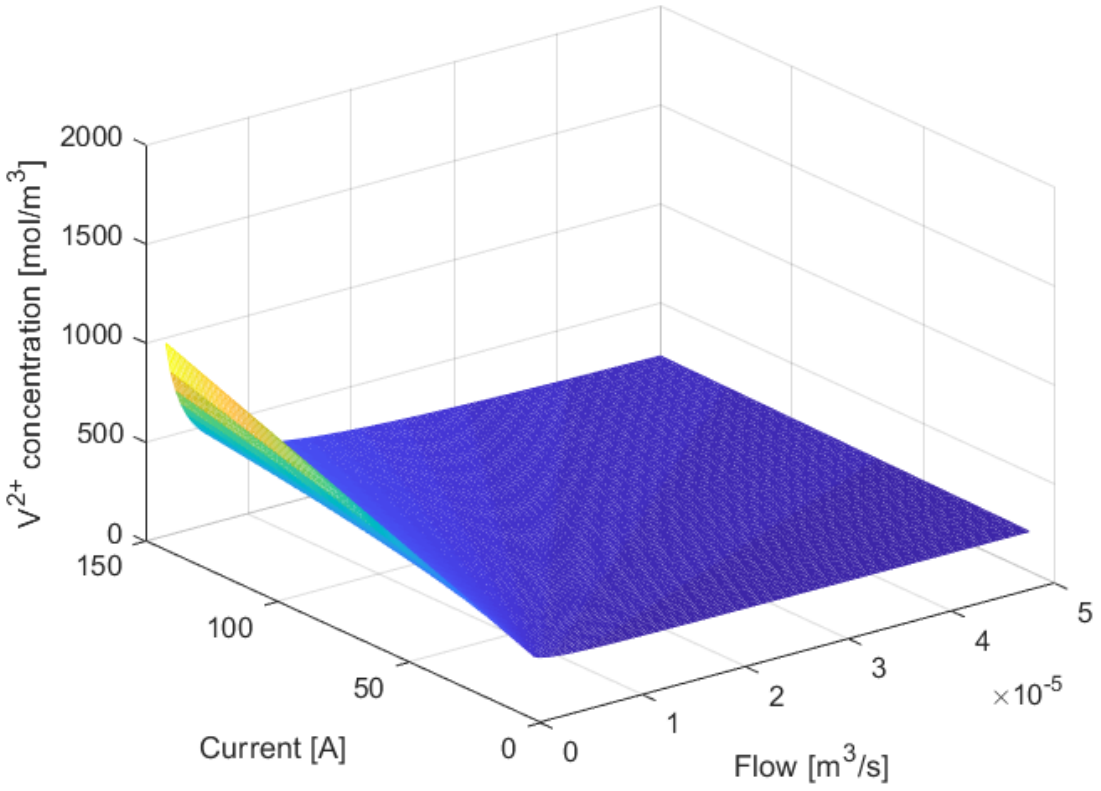

Figure 10. V^{2+} equilibrium points at 10% SOC.

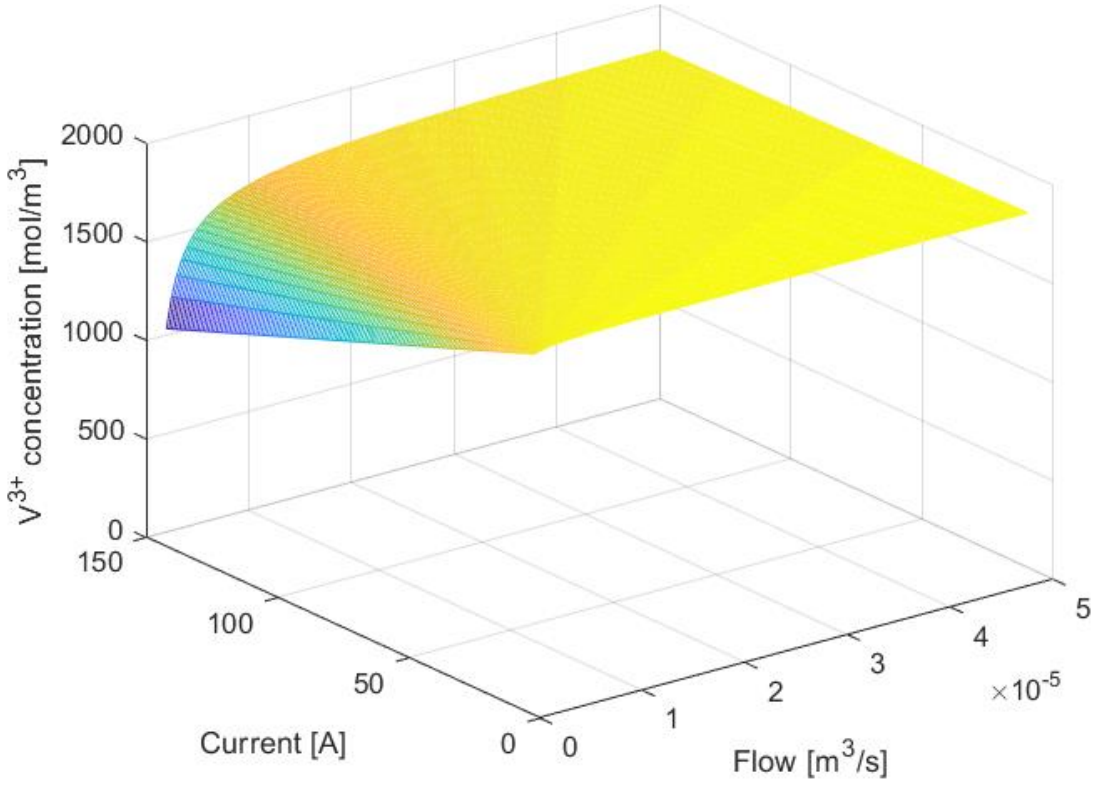

Figure 11. V^{3+} equilibrium points at 10% SOC.

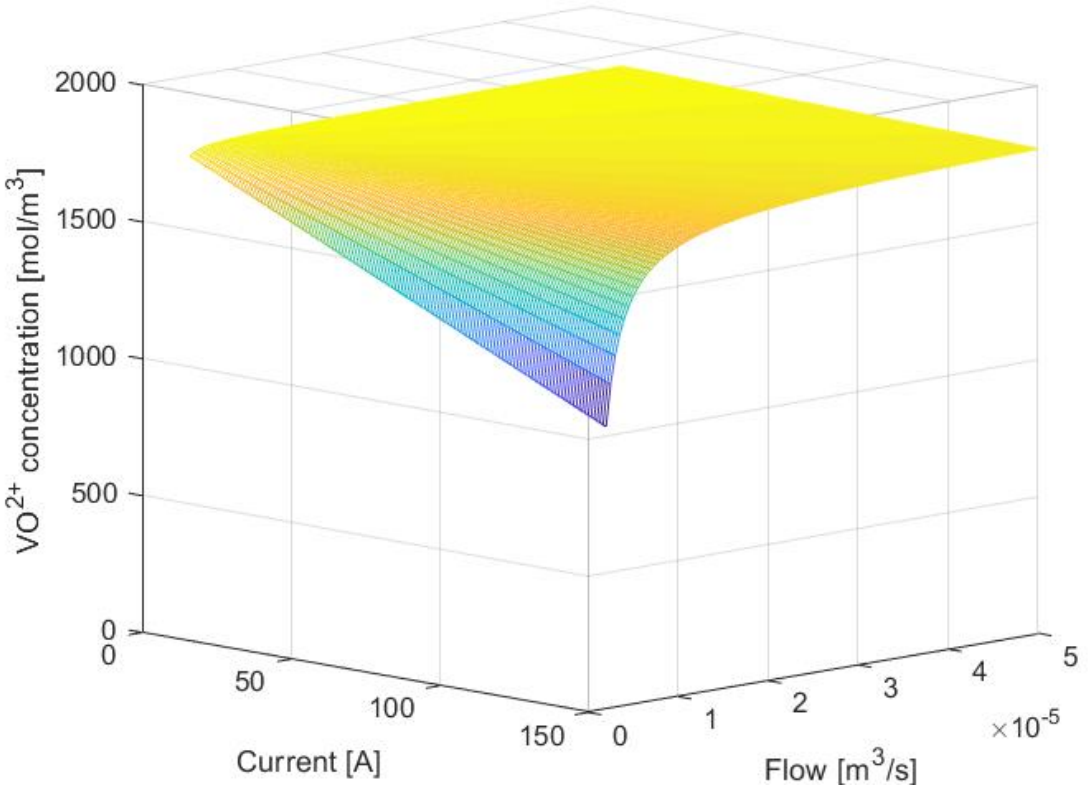

Figure 12. VO^{2+} equilibrium points at 10% SOC.

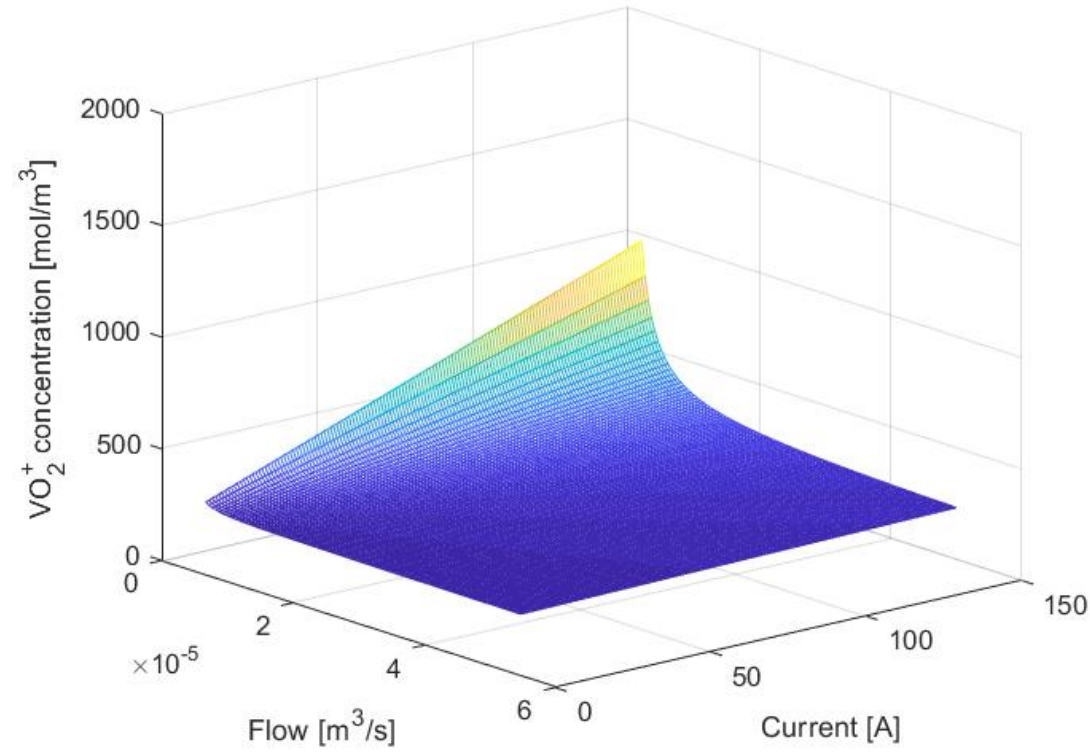

Figure 13. VO_2^+ equilibrium points at 10% SOC.

This first set of surfaces are plotted at a state of charge of 10%, which means that $c_{2,t} = c_{5,t} =$ 200 mol/m^3 and $c_{3,t} = c_{4,t} =$ 1800 mol/m^3.

The mesh stays practically flat at the majority of current and flow points, at a concentration value equal to that of the tank concentration: 200 mol/m^3 in Figure 10 and Figure 11, and 1800 mol/m^3 in Figure 12 and Figure 13. However, at a low enough flowrate, the mesh starts to tilt upwards for the more negative species (V^{2+} and VO_2^+) and upwards for the more positively charged ones (V^{3+} and VO^{2+}), this is especially true as the current goes up. At the highest plotted current and lowest flow, the surface reaches a maximum for Figure 10 and Figure 13 and a minimum for Figure 11 and Figure 12.

The explanation for this is that when the battery is charging at a certain current, the more positively charged ion (for example V^{3+}) will be reduced by the electrons of this positive current, which will convert them to their tank counterparts, the more negatively charged ion (for example V^{2+}). The lower the flow, the more time it will take for the ions in the cell to get out of it. At the same time, the higher the current, the faster this reduction will happen. When these circumstances happen, the consequence ends up being that these reduced ions start to build up in the cell itself, which is why that upwards tilting mentioned in the paragraph before begins to happen in Figure 10 and Figure 13, while the downwards tilting happens at the same time to the counterpart ions in Figure 11 and Figure 12.

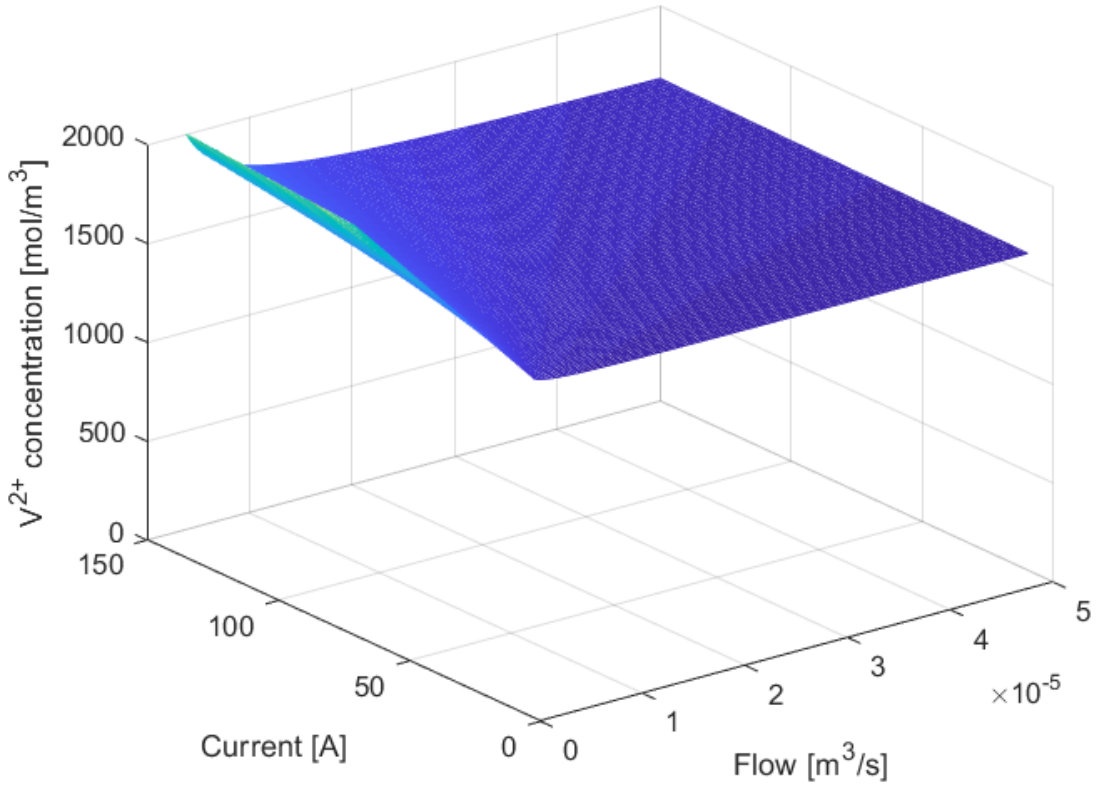

Figure 14. V^{2+} equilibrium points at 80% SOC.

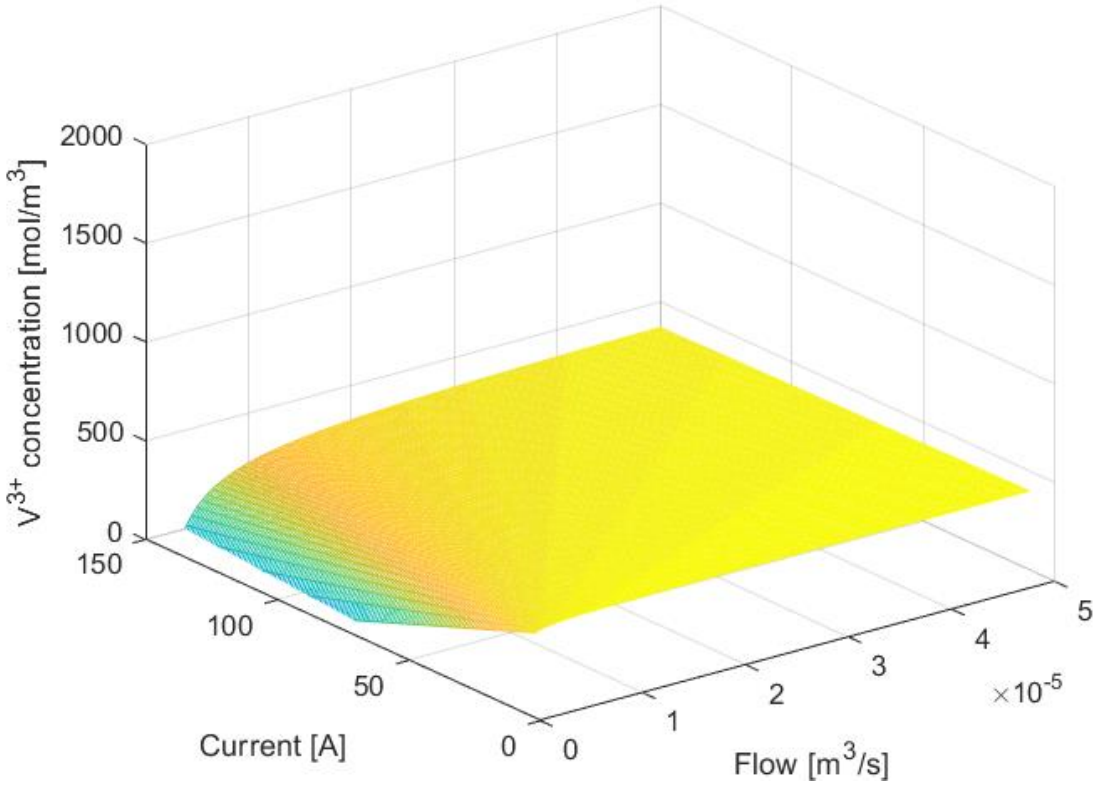

Figure 15. V^{3+} equilibrium points at 80% SOC.

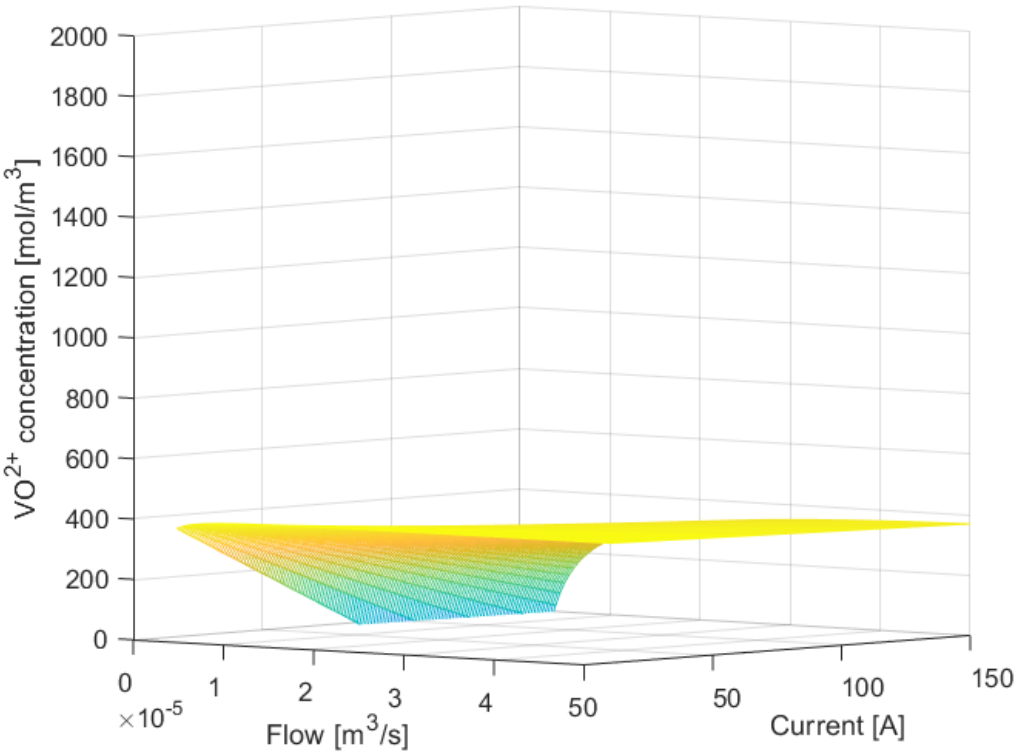

Figure 16. VO^{2+} equilibrium points at 80% SOC.

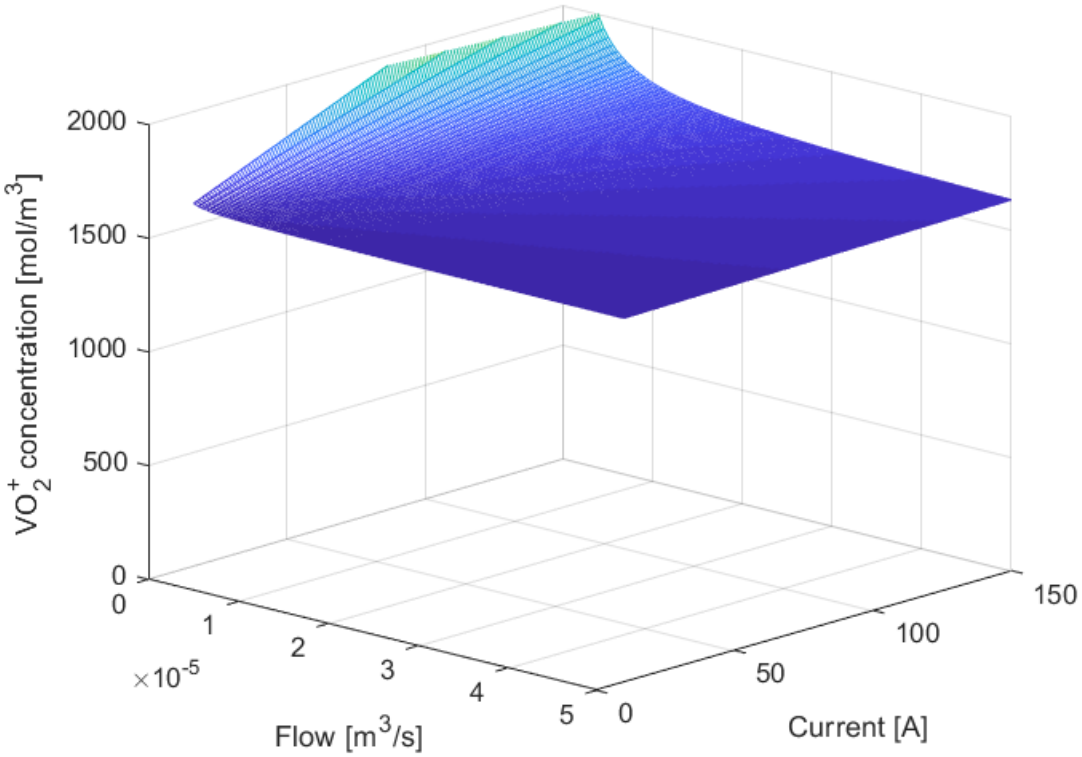

Figure 17. VO_2^+ equilibrium points at 80% SOC.

This first set of surfaces are plotted at a state of charge of 80%, which means that $c_{2,t} = c_{5,t} =$ 1600 mol/m^3 and $c_{3,t} = c_{4,t} =$ 400 mol/m^3.

Just as with the 10% SOC, the mesh stays practically flat at the majority of current and flow points, at a concentration value equal to that of the tank concentration. The behaviour at low flows and high currents is the same as before too. This time it is interesting to observe that the mesh gets cut both at 0 mol/m^3 for Figure 14 and Figure 17, and c_v mol/m^3 for Figure 15 and Figure 16. The equilibrium equations would yield negative values or concentrations higher than c_v if there were no limits established.
The explanation for this is the same one as before: the reduced ions start to build up in the cell when the current is high and/or the flowrate is low.

4.2. Control strategy and influence of SOC

The mathematical model that will be worked with has a lot of variables. Eventually, for the simulation of the model and its controller, the tank concentrations of each species of vanadium will have to be set at a constant value. It is interesting to see how SOC affects the amount of current and flow that need to go through the battery so it can function somewhat optimally.

With some research on the body of work of VRFB models, a control strategy dominates quite a few articles, such as [21], [23], and [24], for example. Equation (6) yields flowrate based on the current, the number of cells in the battery stack, the SOC and the total vanadium concentration of one of the tanks; a parameter defined as flow factor (*FF*) tunes this function and will be set at $FF = 6$ based on article [21].

$$Q_{HC} = FF \cdot \begin{cases} \dfrac{n \cdot I}{F \cdot (1 - SOC) \cdot c_v}, \text{for charging} \\ \dfrac{n \cdot |I|}{F \cdot SOC \cdot c_v}, \text{for discharging} \end{cases} \tag{6}$$

The variable flow rate has been widely used in all the body of work of VRFBs. A low flow rate at the initial and middle processes of charging and discharging satisfies the need for the cell to keep renewing its reactant ions while saving energy. At the extremes of the process, a bigger flowrate is sent to reduce concentration over-potential and fully utilize the maximum capacity of battery [31].

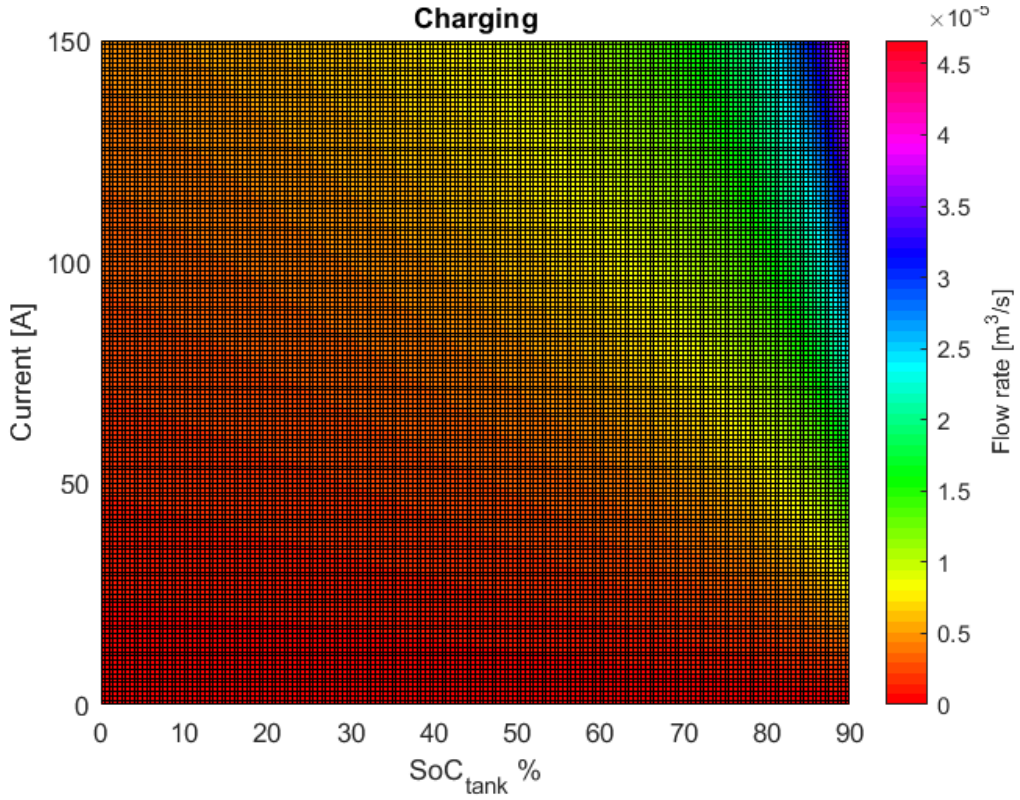

Figure 18. Colourmap of the flowrate when charging the battery using (6).

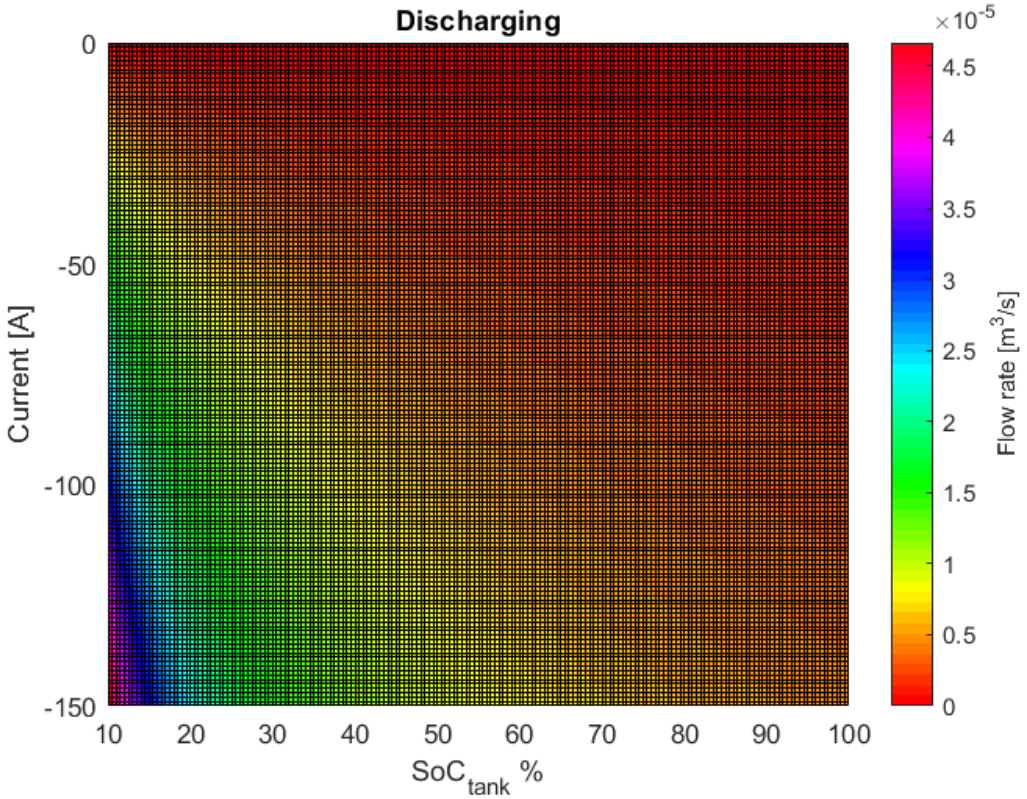

Figure 19. Colourmap of the flowrate when discharging the battery using (6).

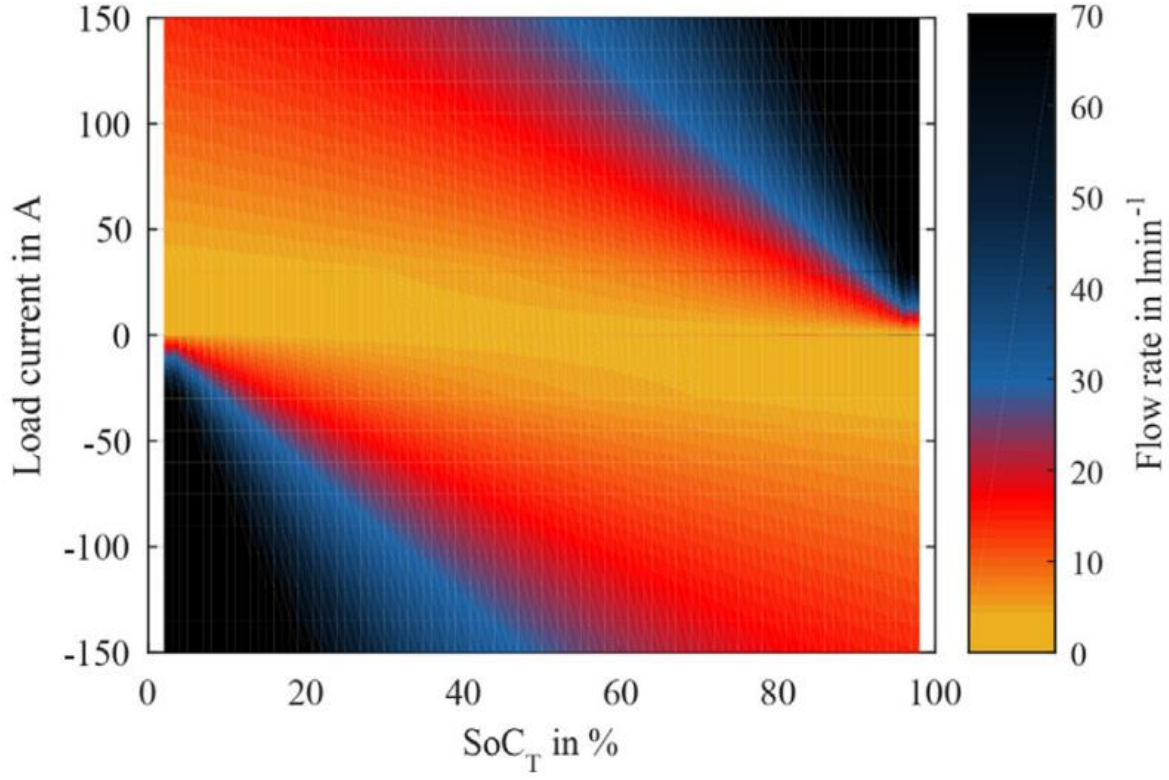

Figure 20. Colourmap of the flowrate in [21].

First off, comparing Figure 18 and Figure 19 with Figure 20, it is observable that the results are very similar. At high SOCs for discharging and low SOCs for charging the calculated flowrate is quite small, especially as the magnitude of the current gets smaller. In contrast, at low SOCs for discharging and high SOCs for discharging and especially as the magnitude of the current goes up, the flowrate begins to increase considerably.

An explanation for these phenomena would be that when charging the battery as in Figure 18, for example, at low SOCs the electrons have a lot of available electrolytes to react with and the need for sending more electron accepting electrolytes is smaller resulting in a lower optimal flowrate. As SOC keeps increasing and less electron gaining species are available, the flow needs to increase in order to give electrons the option to react with the more positively charged electrolytes. Current magnitude magnifies this: more current means a bigger flow of electrons and a sooner expiration of electron accepting species in the cell.

For Figure 19 the explanation is analogue to the one given in the previous paragraph. This time, however, it is the electric circuit that needs electrons to satisfy the current. Thus, at higher SOCs, with the concentration of the cell mostly consisting of the reducer electrolyte (the one that releases electrons), there isn't as much of a need for a high flowrate that keeps on renewing the species of the cell. As SOC decreases, reducer electrolytes do as well, resulting in a bigger needed flowrate to satisfy the amount of current.

It is interesting to see the relationship between the control strategy for the flowrate and the meshes of the equilibrium points found before. The following figures will help to visualize the correspondence at two different SOCs and at different angles.

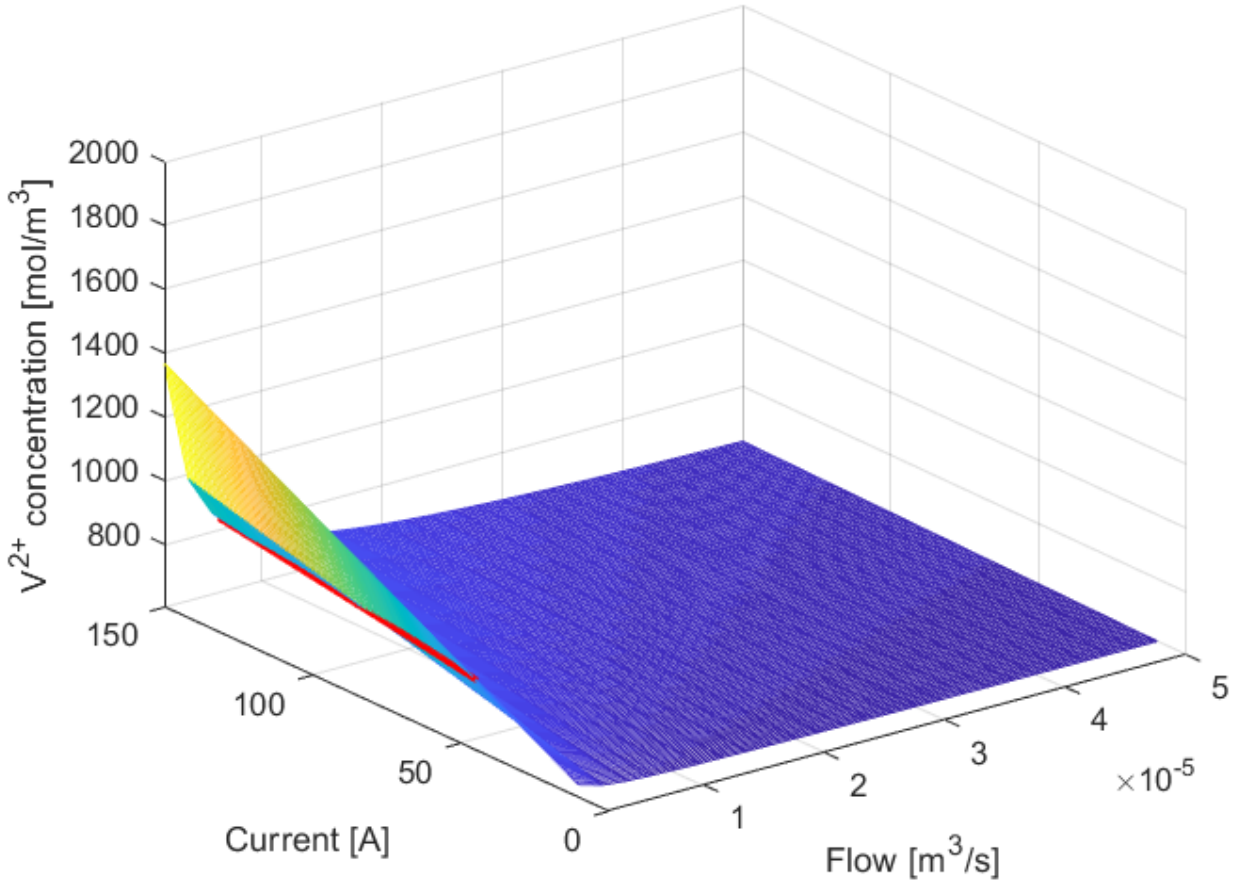

Figure 21. V^{2+} equilibrium points and control strategy (6) at 30% SOC.

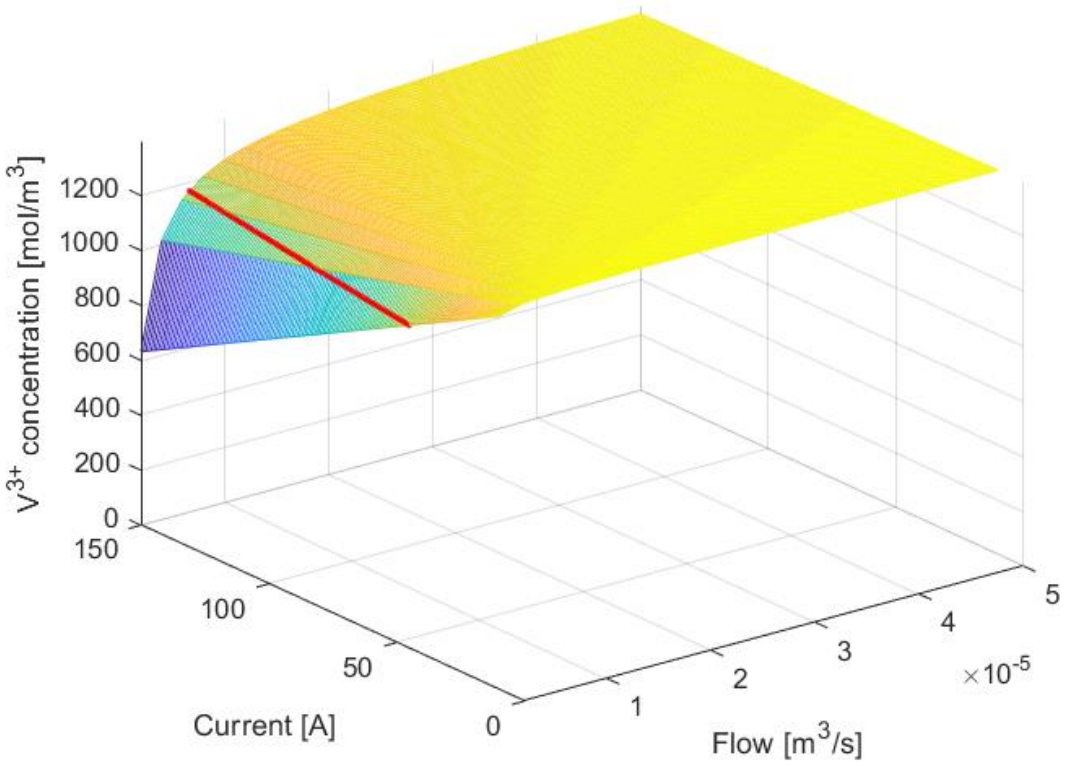

Figure 22. V^{3+} equilibrium points and control strategy (6) at 30% SOC.

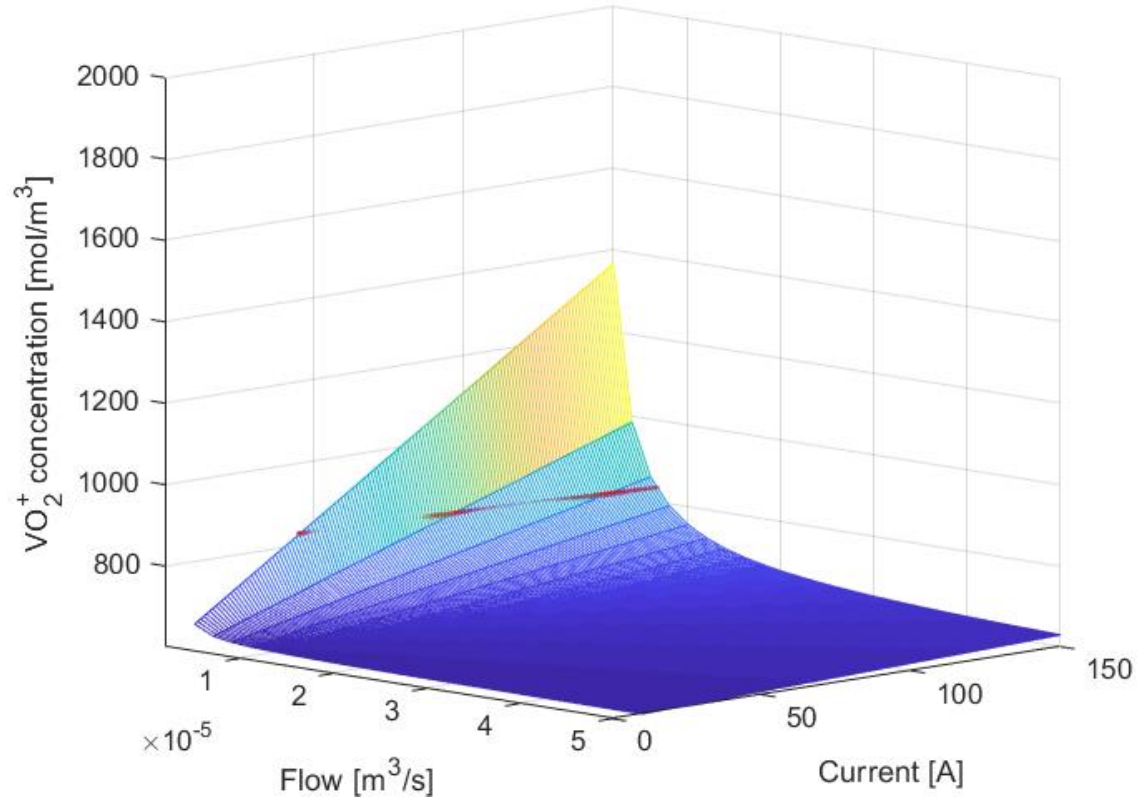

Figure 23. VO_2^+ equilibrium points and control strategy (6) at 30% SOC.

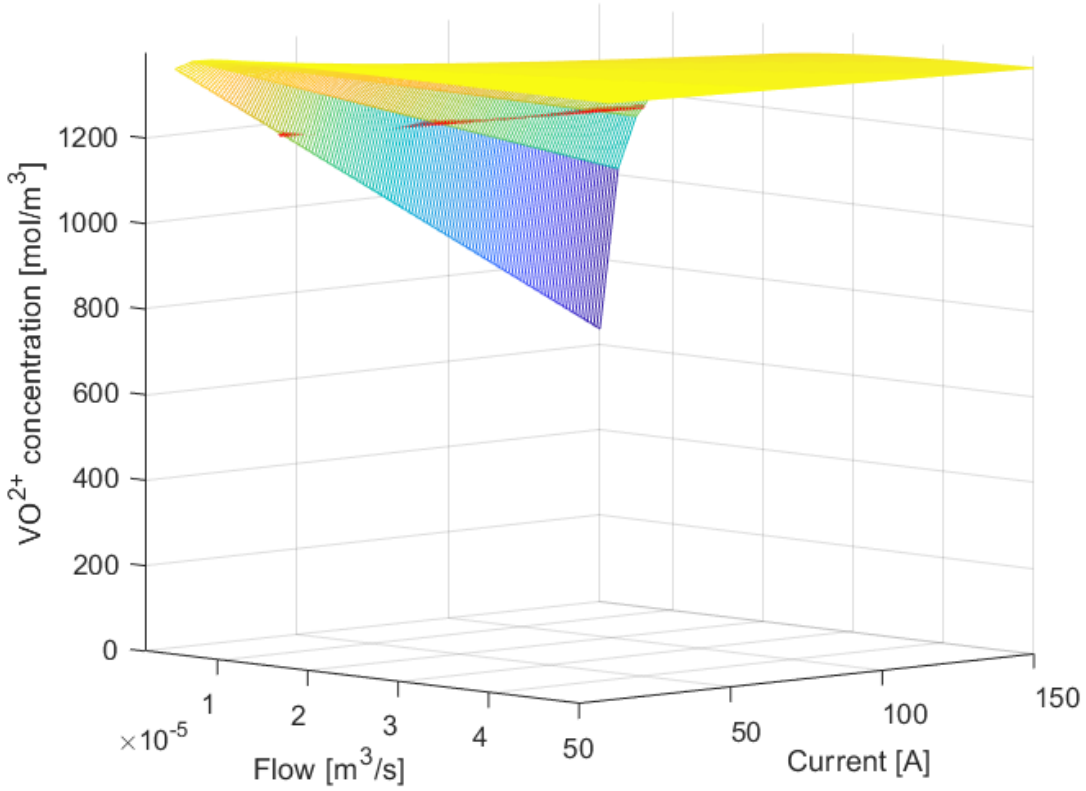

Figure 24. VO^{2+} equilibrium points and control strategy (6) at 30% SOC.

Figure 21, Figure 22, Figure 23 and Figure 24 show how the control strategy function sits inside the equilibrium point mesh as a red line. The figures above are set at 30% SOC which means that $c_{2,t} = c_{5,t} = 600$ mol/m^3 and $c_{3,t} = c_{4,t} = 1400$ mol/m^3.

Figure 21 and Figure 23 as well as Figure 22 and Figure 24 are actually the same plot viewed from a different angle because of how the SOC and tank concentrations are being simplified in this project -as seen in (2)-.

It is interesting to see how it goes beyond the mesh at points that are near the null values of current and flow. These are conflicting points, and in the code used to plot the meshes they have been avoided, if they are not avoided, the surface starts to distort.

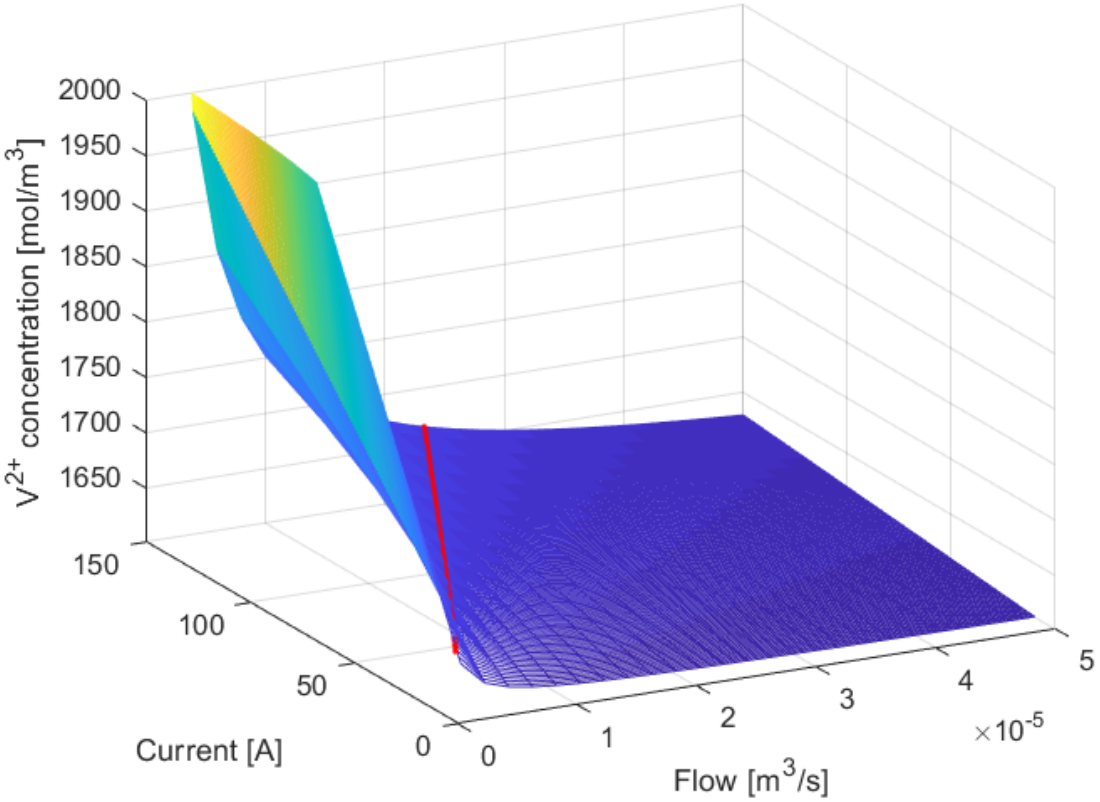

Figure 25. V^{2+} equilibrium points and control strategy (6) at 80% SOC.

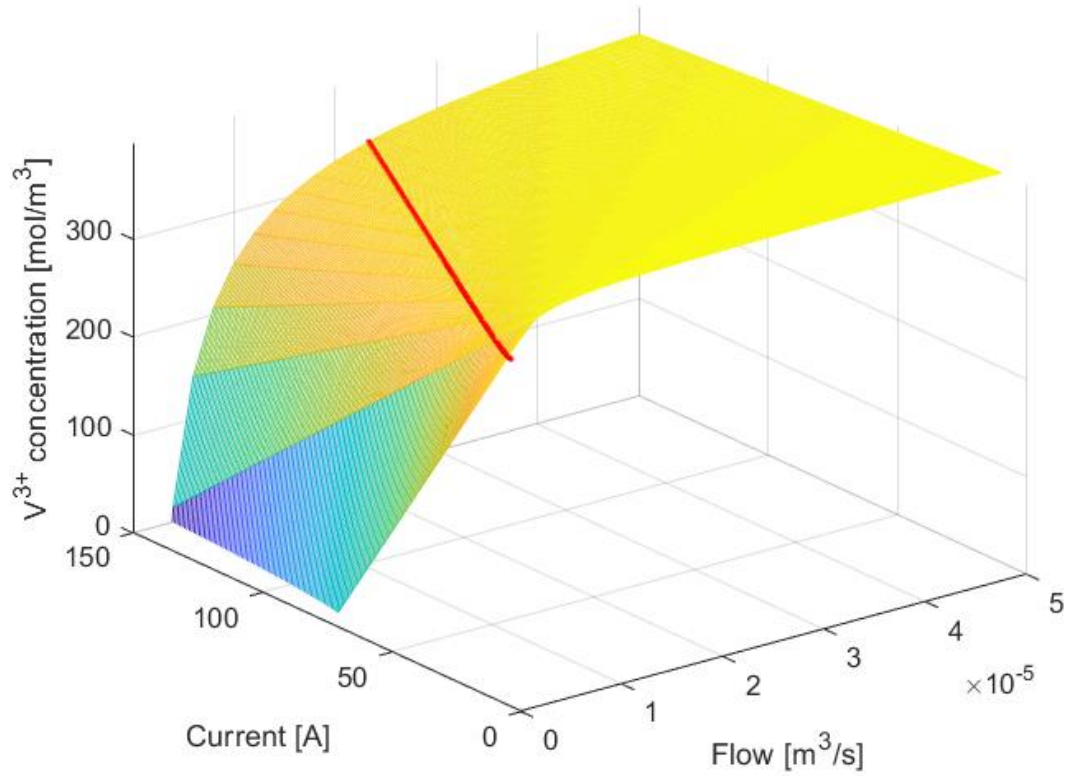

Figure 26. V^{3+} equilibrium points and control strategy (6) at 80% SOC.

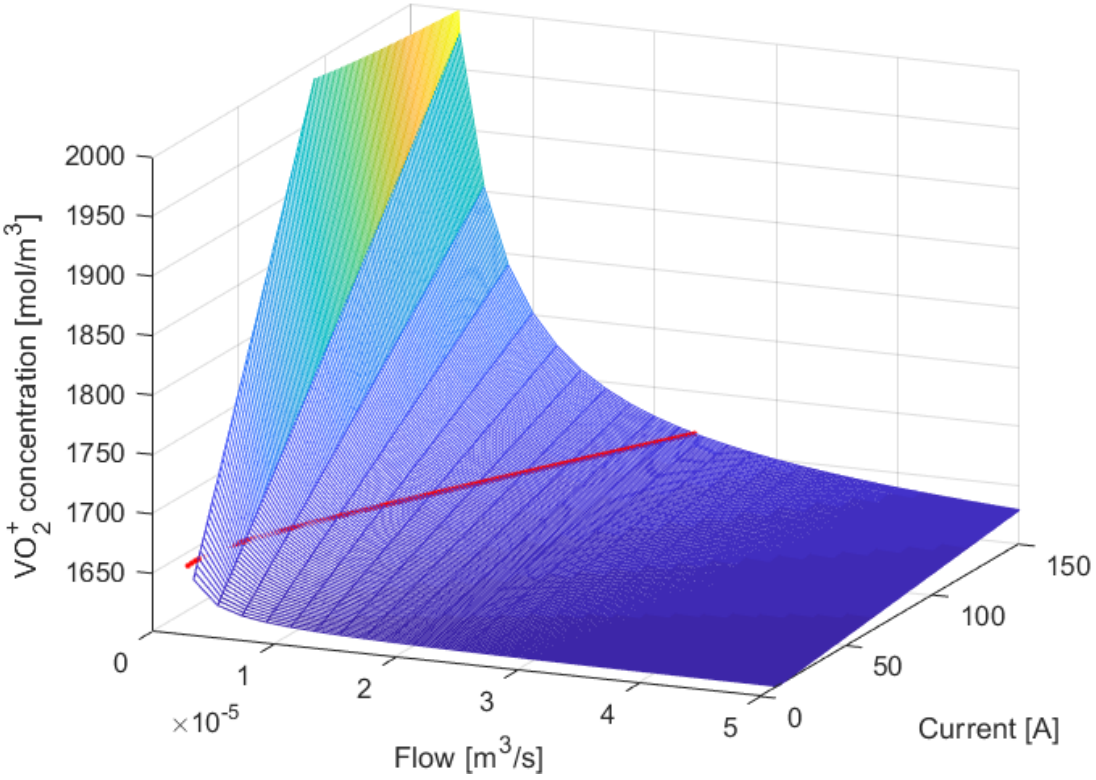

Figure 27. VO_2^+ equilibrium points and control strategy (6) at 80% SOC.

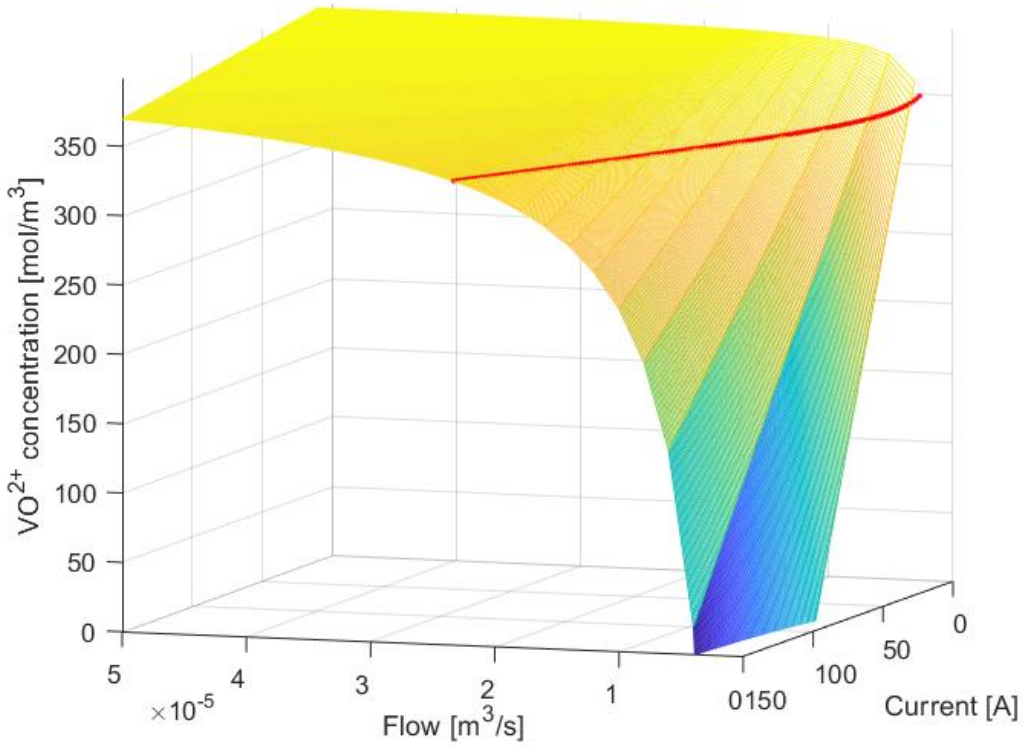

Figure 28. VO^{2+} equilibrium points and control strategy (6) at 80% SOC.

Figure 25, Figure 26, Figure 27 and Figure 28 also show the flowrate control strategy within the mesh plotted with a red line.

The figures above are set at 80% SOC which means that $c_{2,t} = c_{5,t} = 1600$ mol/m^3 and $c_{3,t} = c_{4,t} = 400$ mol/m^3. Again, Figure 25 and Figure 27 as well as Figure 26 and Figure 28 are actually the same plot viewed from a different angle because of how the SOC and tank concentrations are being simplified in this project -as seen in (2)-.

5. CONTROLLER DESIGN

5.1. Theory on system linearization

The procedure to linearize a non-linear system at its equilibrium, such as the plant built from the model described in sections before, is the following [32]:

- Determine an equilibrium operating point $\bar{x}$, $\bar{u}$ for the nonlinear system:

$$\dot{x} = f(x,u); \qquad y = h(x,u)$$

- Define the new variable (equivalent to a small perturbation around the equilibrium)

$$\Delta x = x - \bar{x}; \qquad \Delta u = u - \bar{u}$$

- Considering the Taylor series expansion around $\bar{x}$, $\bar{u}$ (where *h.o.t.* denotes higher order terms):

$$f(x,u) = f(\bar{x},\bar{u}) + \frac{\partial f}{\partial x}\Big|_{\bar{x},\bar{u}} \Delta x + \frac{\partial f}{\partial u}\Big|_{\bar{x},\bar{u}} \Delta u + h.o.t.(\Delta x, \Delta u)$$

- Since $\dot{x} = \Delta\dot{x} + \dot{\bar{x}}$ and if $\Delta x, \Delta u \approx 0$; at an equilibrium point:

$$\Delta\dot{x} \approx \frac{\partial f}{\partial x}\Big|_{\bar{x},\bar{u}} \Delta x + \frac{\partial f}{\partial u}\Big|_{\bar{x},\bar{u}} \Delta u$$

- The same reasoning applies to $h(x,u)$. Now the following approximation can be considered:

$$\Delta\dot{x} = A\Delta x + B\Delta u$$
$$\Delta y = C\Delta x + D\Delta u$$

  where *A*, *B*, *C* and *D* are the state space matrices:

$$A = \frac{\partial f}{\partial x}\Big|_{\bar{x},\bar{u}} \qquad B = \frac{\partial f}{\partial u}\Big|_{\bar{x},\bar{u}} \qquad C = \frac{\partial h}{\partial x}\Big|_{\bar{x},\bar{u}} \qquad D = \frac{\partial h}{\partial u}\Big|_{\bar{x},\bar{u}}$$

This final expression is the linearized system associated with the original system $\dot{x} = f(x,u);\ y = h(x,u)$.

5.2. Linearizing the model

With a plant model built in Simulink (which can be found in the annex) and the equilibrium points equations found before in the project, it is now possible to linearize the plant model around these specific points considering the flowrate as the input, since it is the variable which is the easiest to physically control in real life; and with the battery voltage as the output, which is the variable wanted to be set at a concrete reference value.

For that purpose, the MATLAB function *linmod()* comes in handy. It allows for the linearization of a specific Simulink file at an operating point that can be manually set, and it returns the state space matrices *A*, *B*, *C* and *D* mentioned in the procedure from before. From this yielded state space representation another MATLAB function, *ss2tf()*, converts the state space model with the matrices as the input to a continuous transfer function.

This procedure is done throughout various equilibrium points that come from iterating at SOC values from 10% to 90% in steps of 20% and, at each of these charges, iterating the current from 10 A to 150 A in steps of 20 A.

The transfer functions resulting from each of these points are plotted in a Bode plot to see how the behaviour of the plant changes at different conditions.

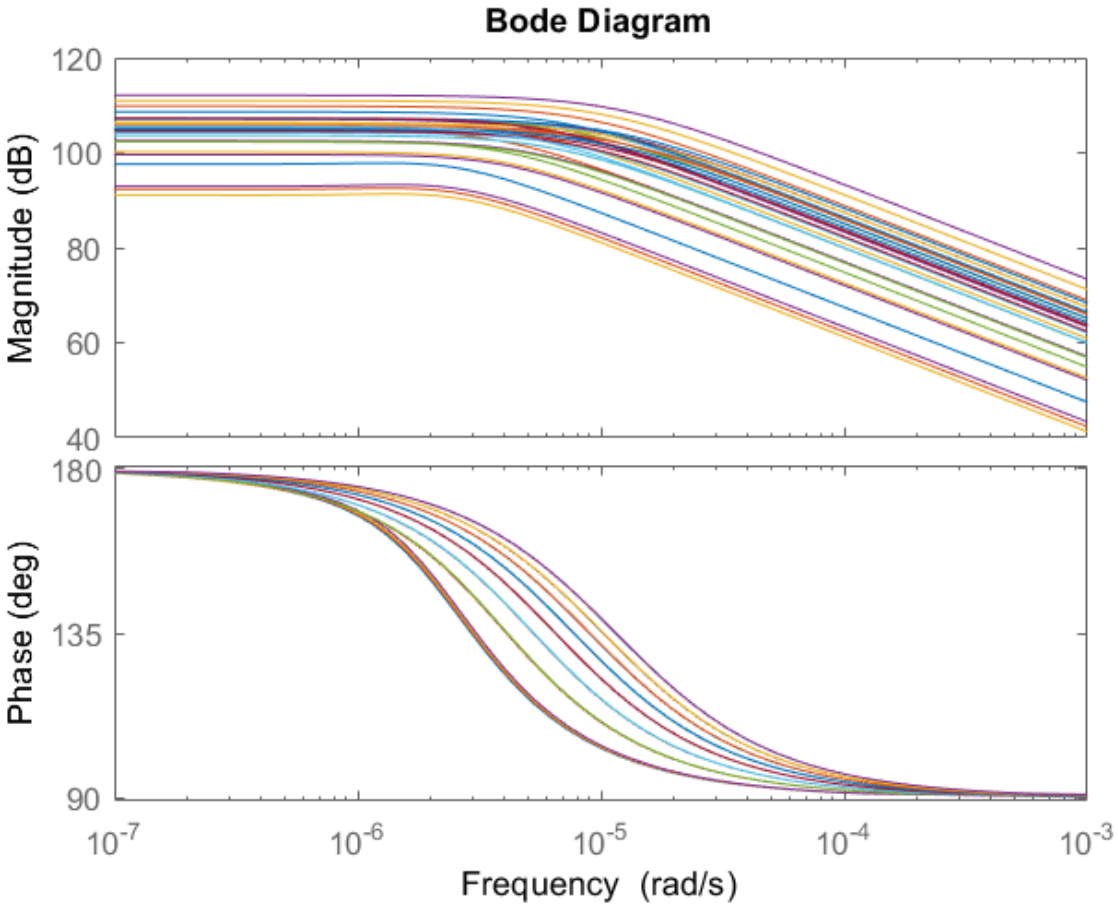

Figure 29. Bode plots for all the transfer functions at the evaluated points.

From the bode plot it is possible to observe that the behaviour is quite similar at all the different evaluated points. It seems that a single type of controller could be sufficient for the control of the plant. The MATLAB function *minreal()* simplifies the poles and zeros of the system that are very similar with a relative tolerance that can be set.

To be sure of the results, a Bode plot of the simplified functions is now drawn.

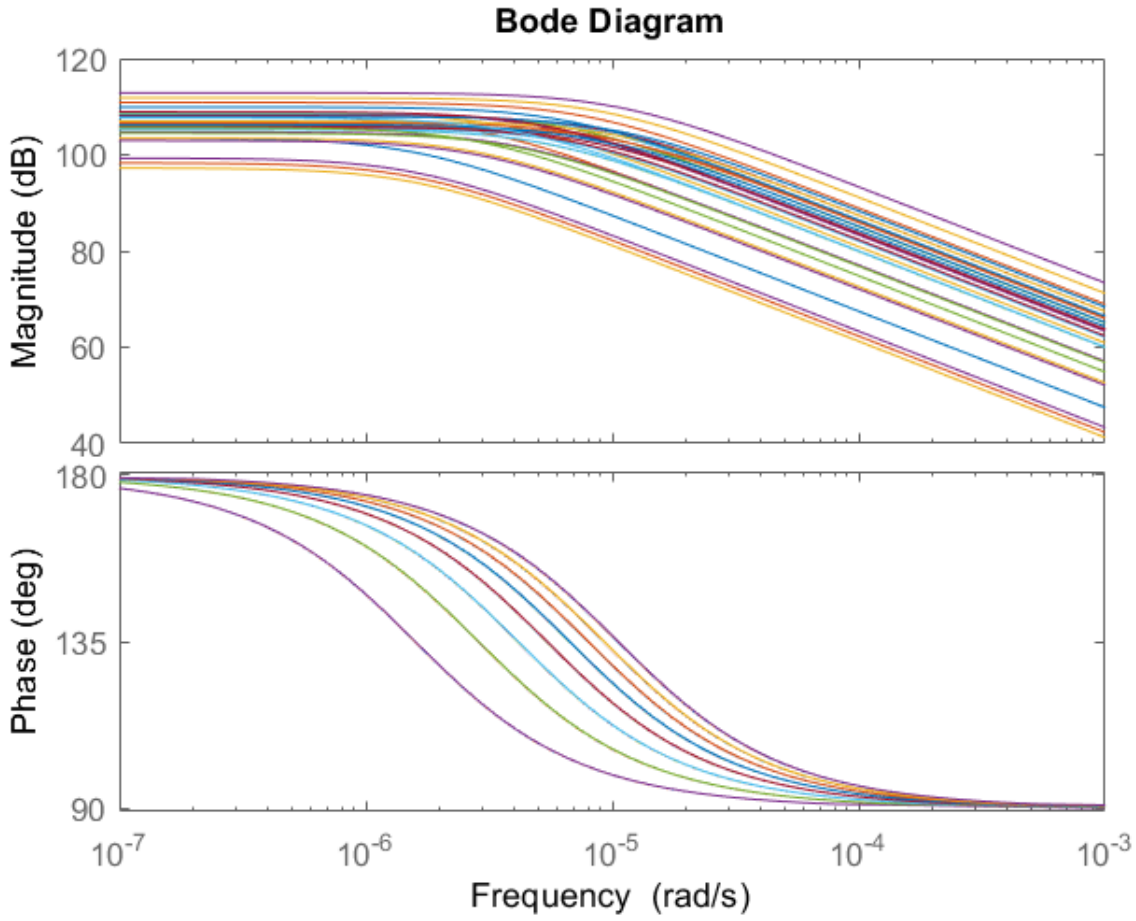

Figure 30. Bode plots for the simplified transfer functions with tolerance ε = 10-3.

Comparing Figure 29 and Figure 30, the differences are almost unappreciable. For this reason, a first order system will be used to design the controller. It will be a PI (proportional and integral controller) with feedback.

5.3. PI design

A generic first order transfer function can be written as:

$$P(s) = \frac{K}{\tau s + 1} \tag{7}$$

where *K* is the DC gain, which is the ratio of the magnitude of the steady-state step response to the magnitude of the step input; and τ is the time constant, which is equal to the time it takes for the system's response to reach approximately 63% of its steady-state value for a step input.

A generic PI controller transfer function can be written as:

$$C(s) = \frac{Kp \cdot s + Ki}{s} \tag{8}$$

Where *Kp* is the proportional constant and *Ki* is the integral constant.

A PI controller with feedback allows for the modification of the *K* and τ constants of a plant in the following way:

- First, a schematic of how the complete system will look like with the controller:

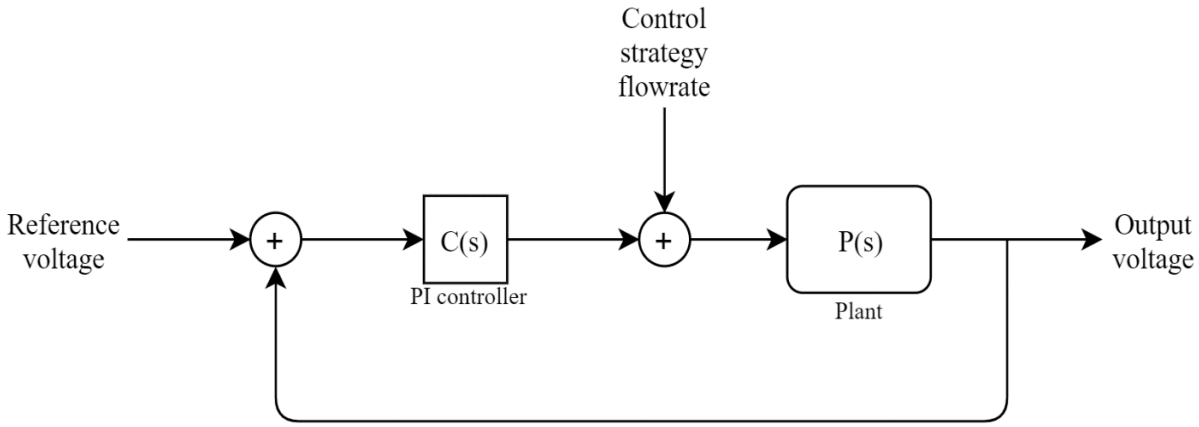

Figure 31. Schematic of the whole system.

- Interpreting the controller as the following function:

$$C(s) = \frac{Q(s)}{1 - Q(s) \cdot P(s)}$$

- Defining the new desired time constant τ^*, and in order to substitute the original one τ by the new one:

$$Q(s) \cdot P(s) = \frac{K}{\tau s + 1} \cdot \frac{\tau s + 1}{(\tau^* s + 1) \cdot K} = \frac{1}{\tau^* s + 1}$$

- Coming back to *C(s)*:

$$\boldsymbol{C(s)} = \frac{Q(s)}{1 - Q(s) \cdot P(s)} = \frac{\frac{\tau s + 1}{(\tau^* s + 1) \cdot K}}{1 - \frac{1}{\tau^* s + 1}} = \frac{\frac{\tau s}{K} + \frac{1}{K}}{\tau^* s} = \frac{\frac{\boldsymbol{\tau}}{\boldsymbol{\tau^* K}} \boldsymbol{s} + \frac{\mathbf{1}}{\boldsymbol{\tau^* K}}}{\boldsymbol{s}}$$

- Comparing *C(s)* with the generic PI function:

$$C(s) = \frac{\frac{\tau}{\tau^* K} s + \frac{1}{\tau^* K}}{s} = \frac{Kp \cdot s + Ki}{s}$$

Thus,

$$\boldsymbol{Kp = \frac{\tau}{\tau^* K}} \qquad \boldsymbol{Ki = \frac{1}{\tau^* K}}$$

Having the algebraic expressions for the controllers allows the controller to be dependent of the conditions of the simulation, at least the ones that it starts with.

To do so, a MATLAB script -that is also responsible for setting up all the constants in the Simulink model- determines the equivalent transfer function of the plant at a specific operating point. Then, from the transfer function the DC gain *K* and the time constant τ are calculated and, with a desired time constant, the *Kp* and *Ki* values are set. Considering that the largest τ of all the calculated transfer functions have a magnitude order of 6 digits, τ^* will be set at a magnitude order of about 3 digits.

5.4. Simulations

As a reminder, these are the constants that will not change in any of the simulations because they are either scientific constants, part of the design or aspects decided not to be regarded thoroughly:

Table 3. Simulation constants

Cells in the stack	$\boldsymbol{n} = 40$
Flow factor	$\boldsymbol{FF} = 6$
Formal voltage	$\boldsymbol{E_{formal}} = 1.4$ [V]
Cell active area	$\boldsymbol{A_C} = 0.02$ [m^2]
Ionic membrane thickness	$\boldsymbol{d_M} = 1.27 \cdot 10^{-4}$ [m]
Total vanadium tank concentration	$\boldsymbol{c_v} = 2 \cdot 10^{3}$ [mol/m^3]
Diffusion coefficients	$\boldsymbol{D_2} = 4.4380 \cdot 10^{-12}$ [m^2/s] $\boldsymbol{D_3} = 1.0024 \cdot 10^{-12}$ [m^2/s] $\boldsymbol{D_4} = 3.8000 \cdot 10^{-12}$ [m^2/s] $\boldsymbol{D_5} = 1.7500 \cdot 10^{-12}$ [m^2/s]
Half-cell volume	$\boldsymbol{V_{HC}} = 6.1 \cdot 10^{-3}$ [m^3]
Tank volume	$\boldsymbol{V_{tank}} = 12.36$ [m^3]
Temperature	$\boldsymbol{T} = 298$ [K]
Ideal gas constant	$\boldsymbol{R} = 8.31$ [J/(mol·K)]
Faraday constant	$\boldsymbol{F} = 96485$ [C/mol]
Desired time constant	$\boldsymbol{\tau^*} = 240$ [s]

The model for the whole system can be seen in the annex. It is important to remember that, although for the original plant model the tank concentrations' evolution was not considered, the model of the whole system contains a small add-on that yields the change of tank concentrations through time (and therefore, also the SOC). Since it is assumed that the rate of change is very slow, this small addition should not have much of an impact on the results.

5.4.1. First simulation – Varying voltages

As a start and to check the reliability of the model, a first simulation with a variable reference voltage will be carried out.

The state of charge will start at SOC = 60% and the current will be constant at I = 80 A.

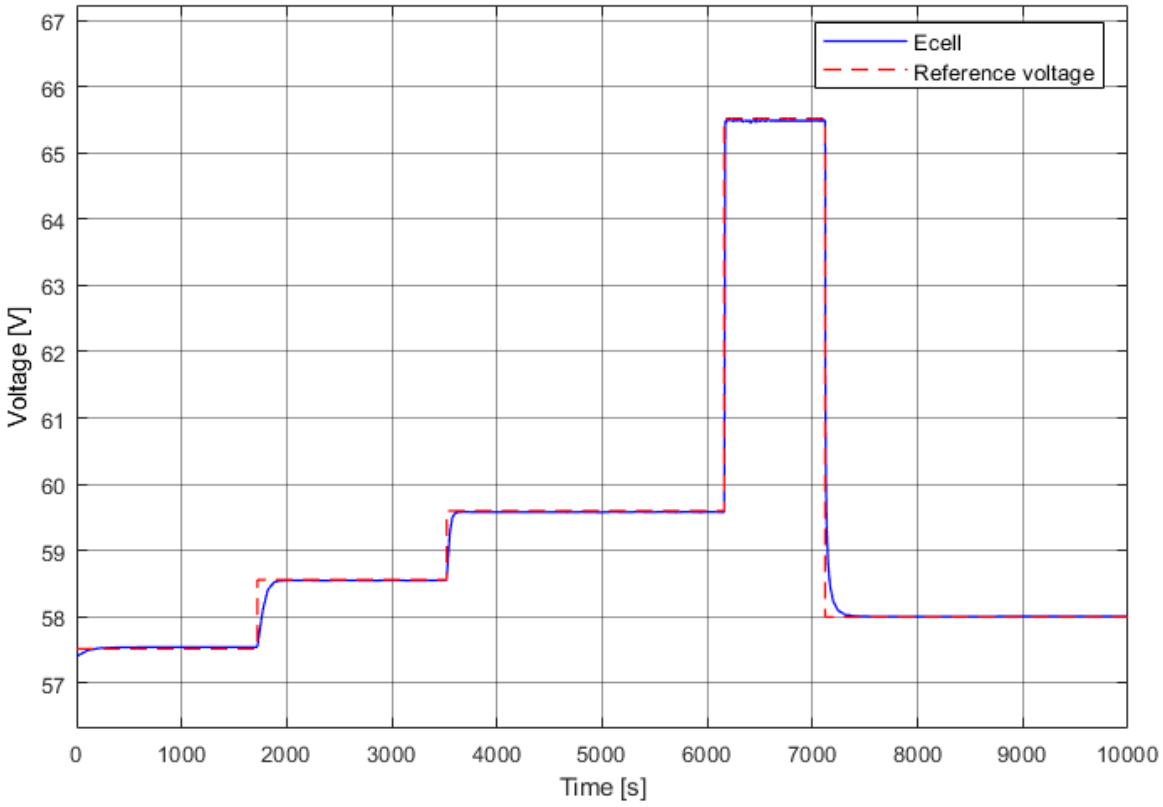

Figure 32. First simulation's output voltage and reference voltage.

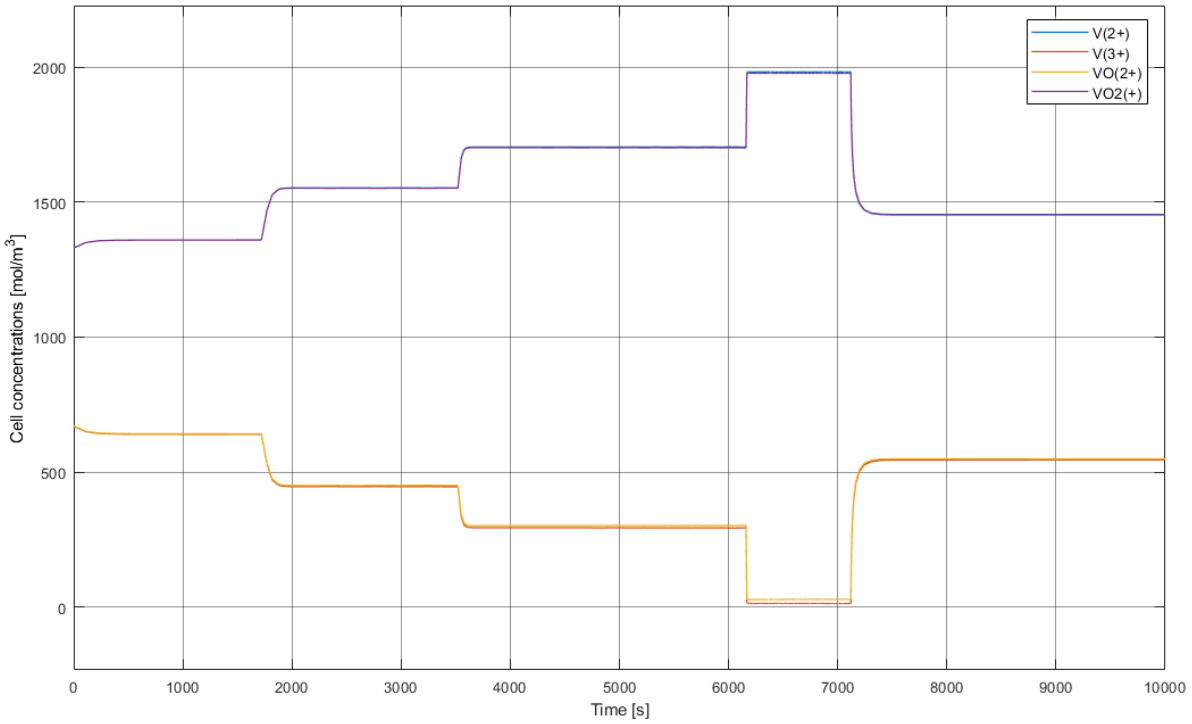

Figure 33. First simulation's cell concentrations.

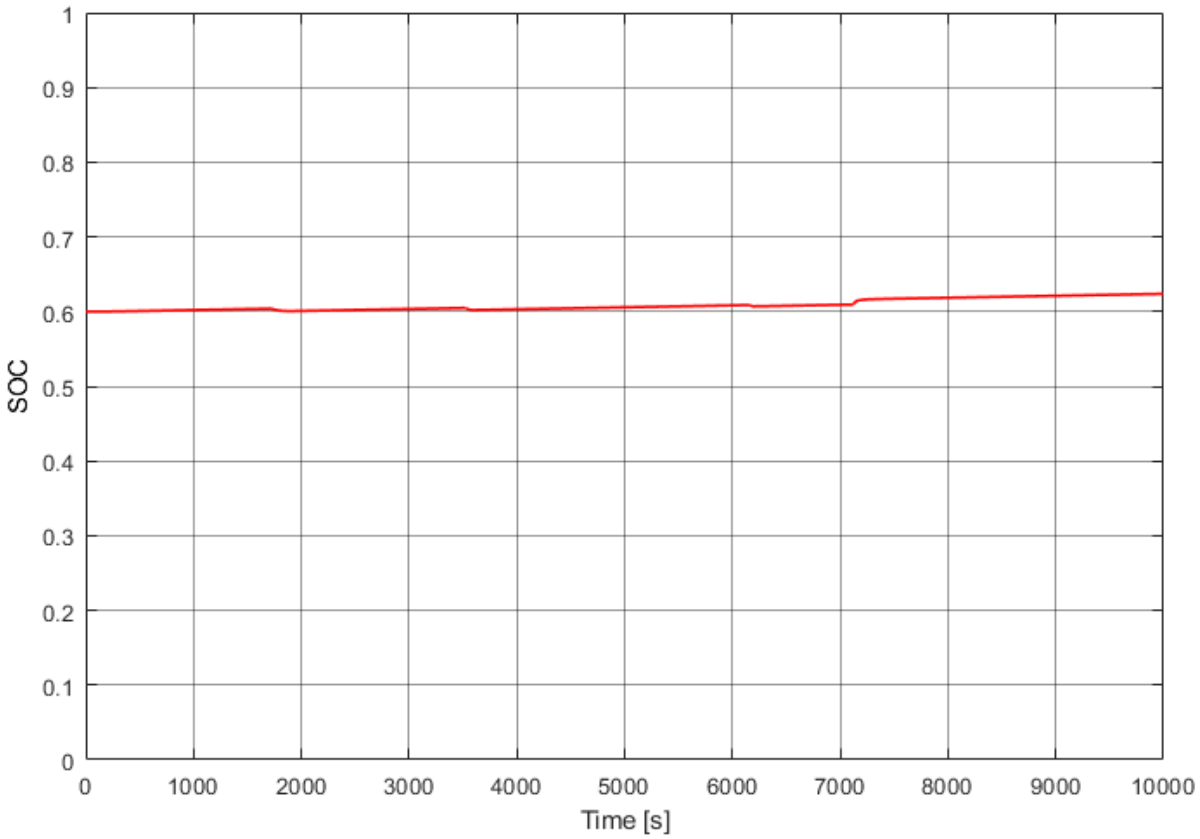

Figure 34. First simulation's state of charge.

In Figure 32 the system responds fast and well to the voltage reference even at the highest peak which is equivalent to a voltage at all the cells 1.65V, this is the value that was used to calculate the number of cells in the stack that could deliver the maximum power to the house imagined in section 3.4.

Figure 33 shows how the concentrations in the cell keep on changing. The negative ions of both tanks keep increasing as the reference voltage does so, when this voltage decreases at the end, the negative ions also go down. It is interesting to see how the concentration of their counterpart ions evolve symmetrically.

Figure 34 displays the state of charge that very slowly goes up, proving that the decision to assume the tank concentration constant throughout time is indeed reasonable. It also is in concordance with the positive current which indicates that the battery is being charged. If looked at closely and with Figure 33, the SOC suffers tiny jumps at points of fast cell concentration changes.

5.4.2. Second simulation – Varying consumption

For the second simulation it is interesting to see how the battery would behave when it had to supply energy to a house. The reference voltage will be kept constant at a value of 60 V and the state of charge will start at 60%.

A random signal will be taken as the input current to replicate the variation of power that the house requires. A moment with a high module current could represent an electric car being plugged in or the AC being turned on; a moment with a low module current could represent all the lights of the house being turned off at night or the disconnection of the fridge in order to clean it.

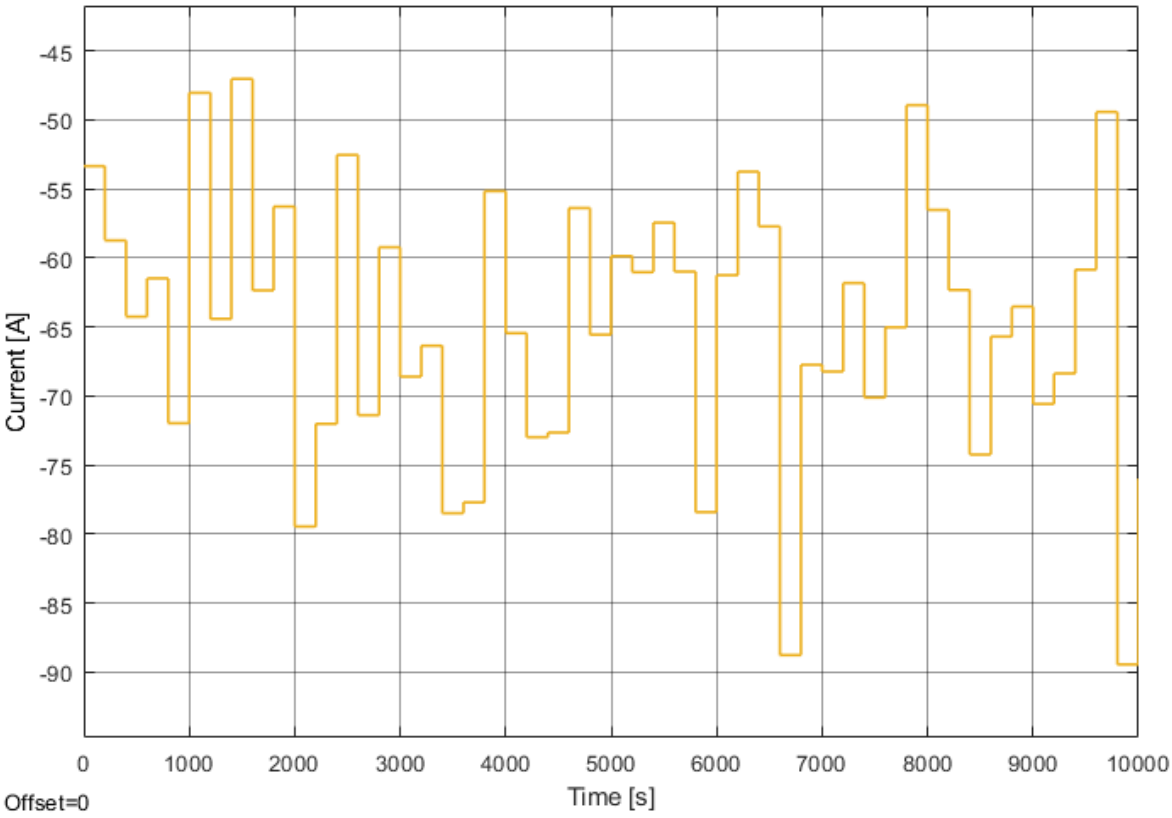

Figure 35. Second simulation's input current.

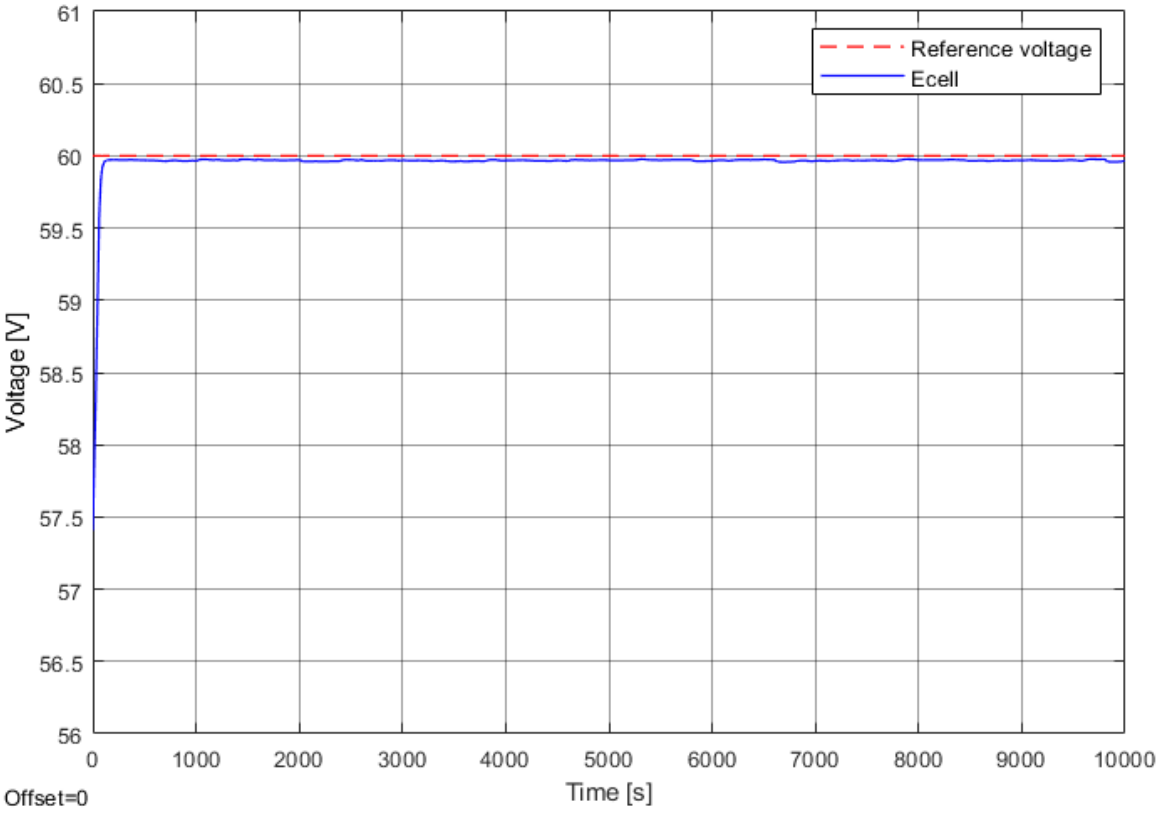

Figure 36. Second simulation's output voltage and reference voltage.

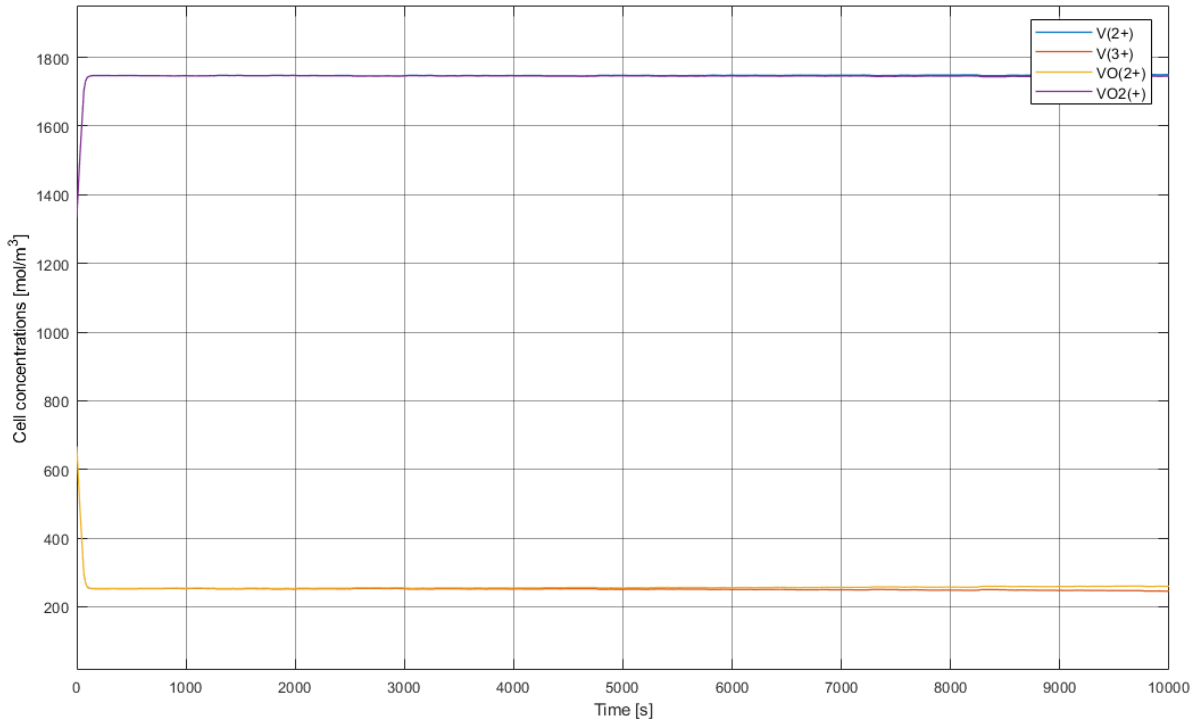

Figure 37. Second simulation's cell concentrations.

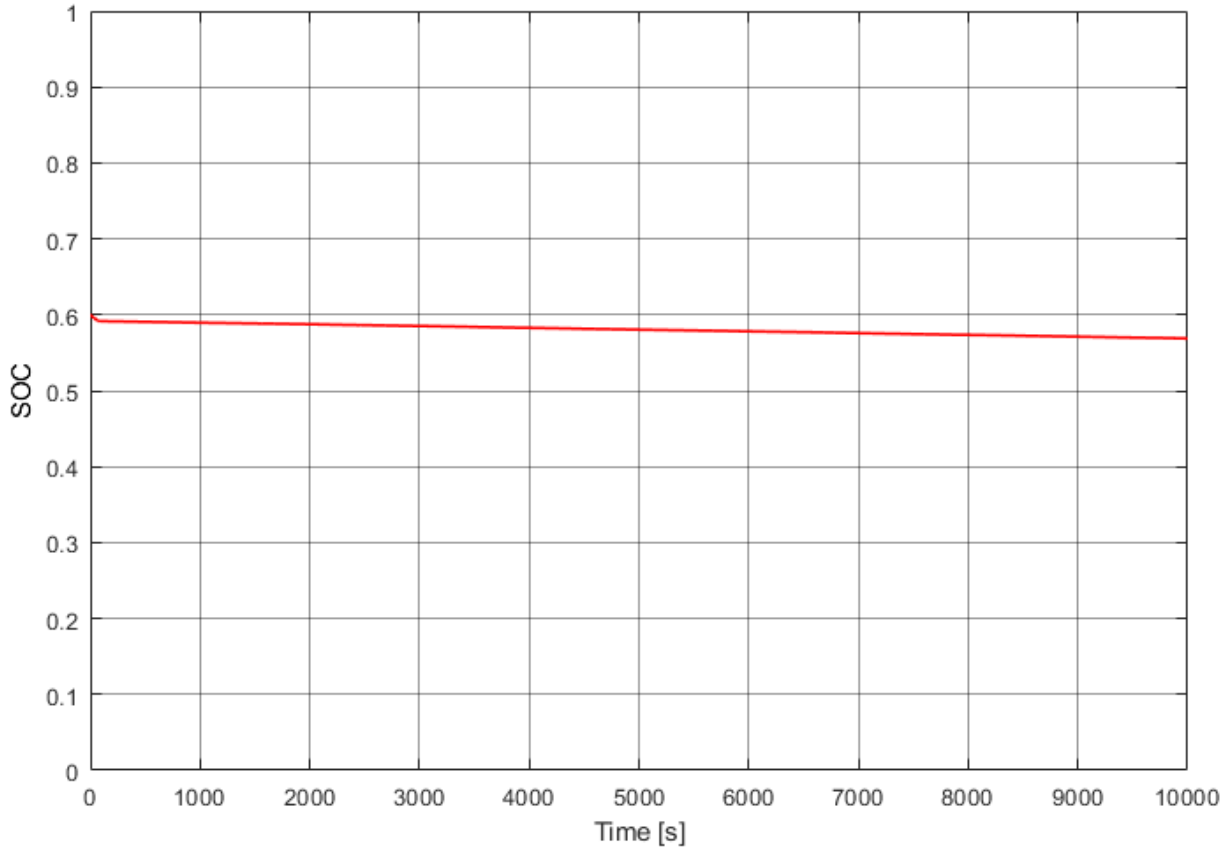

Figure 38. Second simulation's state of charge.

Figure 35 shows the random signal generated with a Simulink block. The rate and range of the current change is probably quite exaggerated, but it is interesting to see how the system reacts to those quick fluctuations.

The voltages in Figure 36 coincide throughout time, which is a good sign, as it shows that the controller is able to keep on delivering the desired electric potential.

The cell currents in Figure 37 are quite steady once the reference voltage is achieved.

Figure 38 shows the slow depletion of the battery as time goes by. In contrast to the first simulation, the decrease in the state of charge is very smooth.

5.4.3. Third simulation – Positive and negative currents

In this third and last simulation there are two limitations to remember: firstly, all the work has been done under the assumption that the tank concentrations change at a really slow pace; and secondly, the model does not behave well at neither very high nor very low states of charge. For these reasons, the simulation will be conducted with a sinusoidal current with very low frequency that moves between positive and negative currents.

The reference voltage is set once again at a constant 60 V and the initial state of charge is 30%.

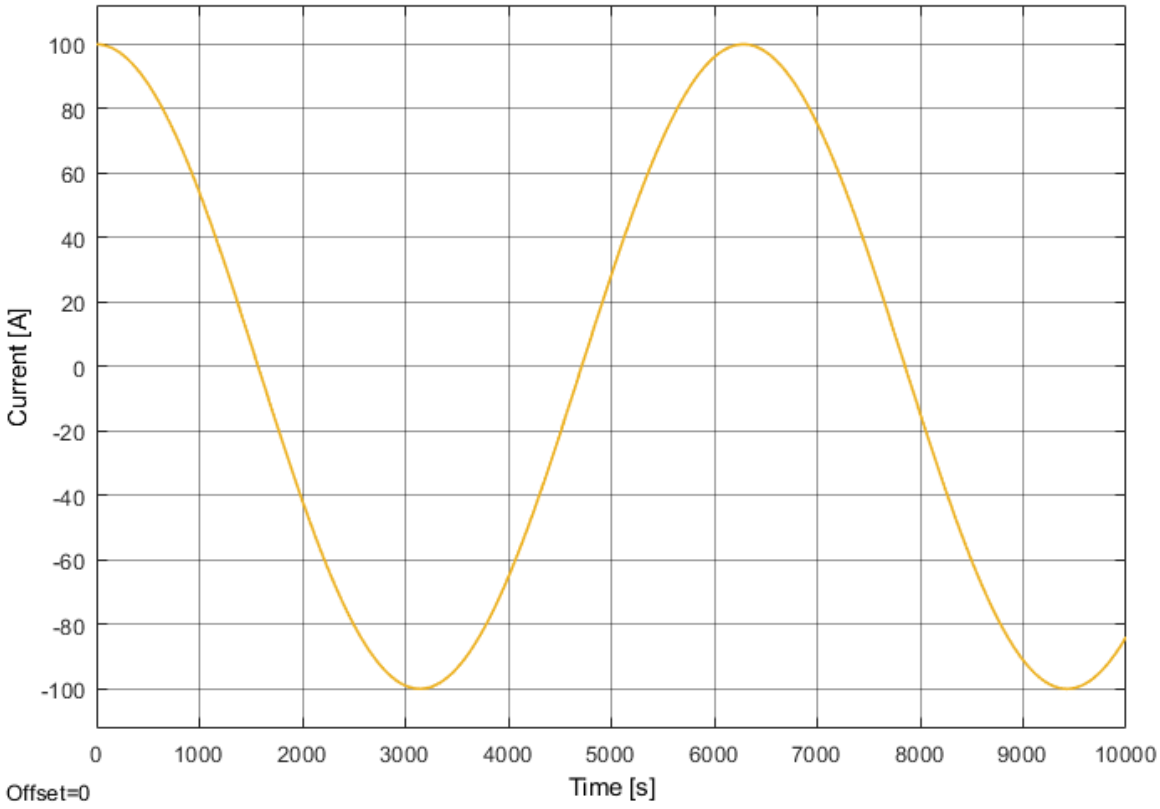

Figure 39. Third simulation's input current.

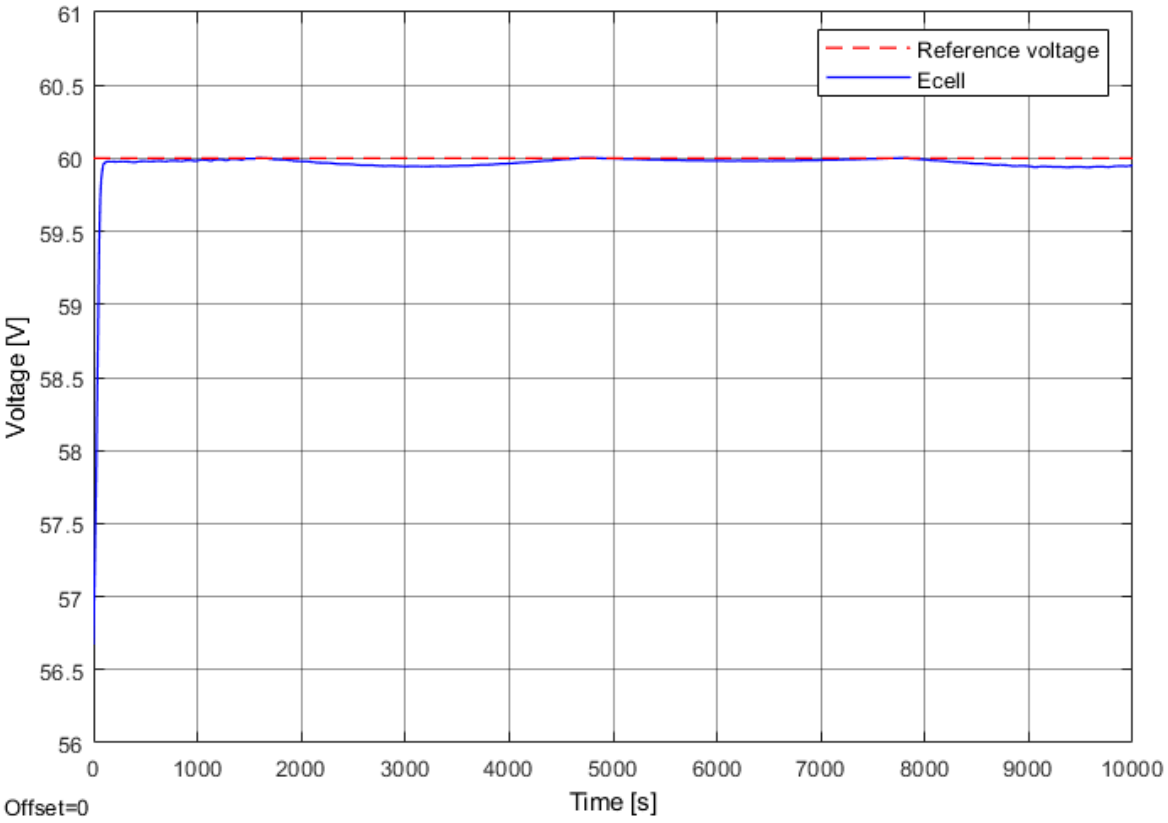

Figure 40. Third simulation's output voltage and reference voltage.

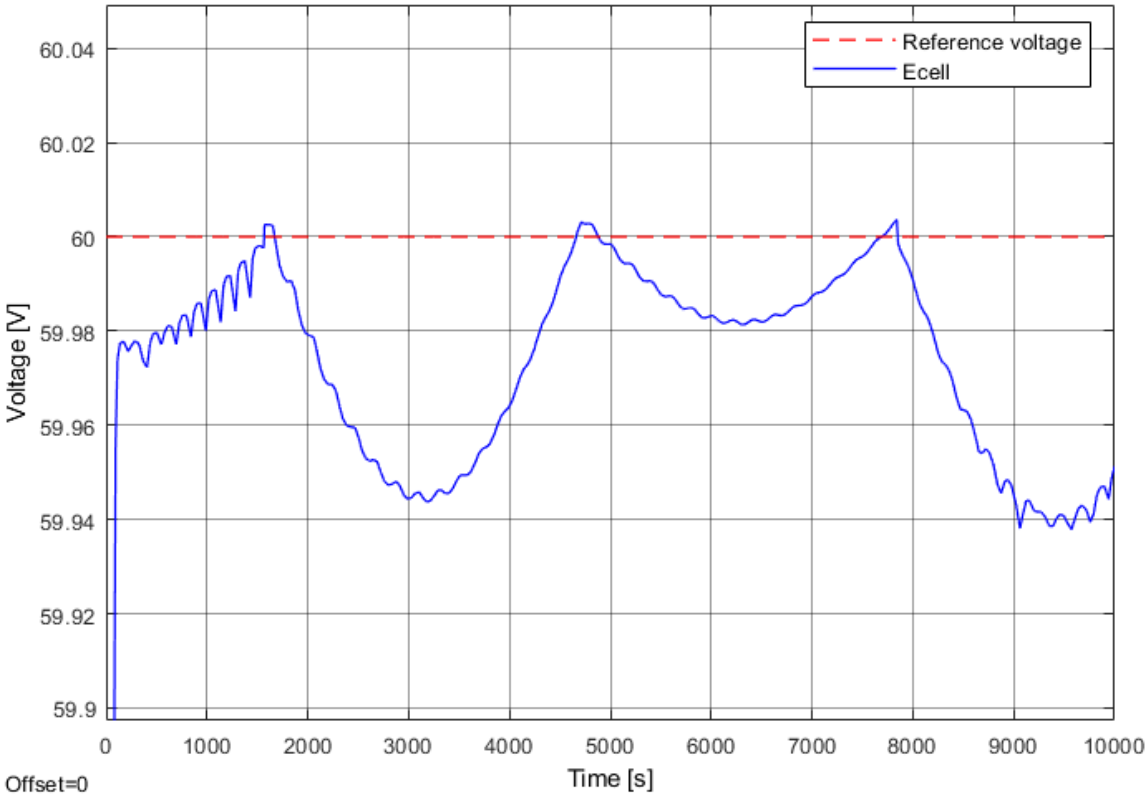

Figure 41. Third simulation's zoomed-in output voltage.

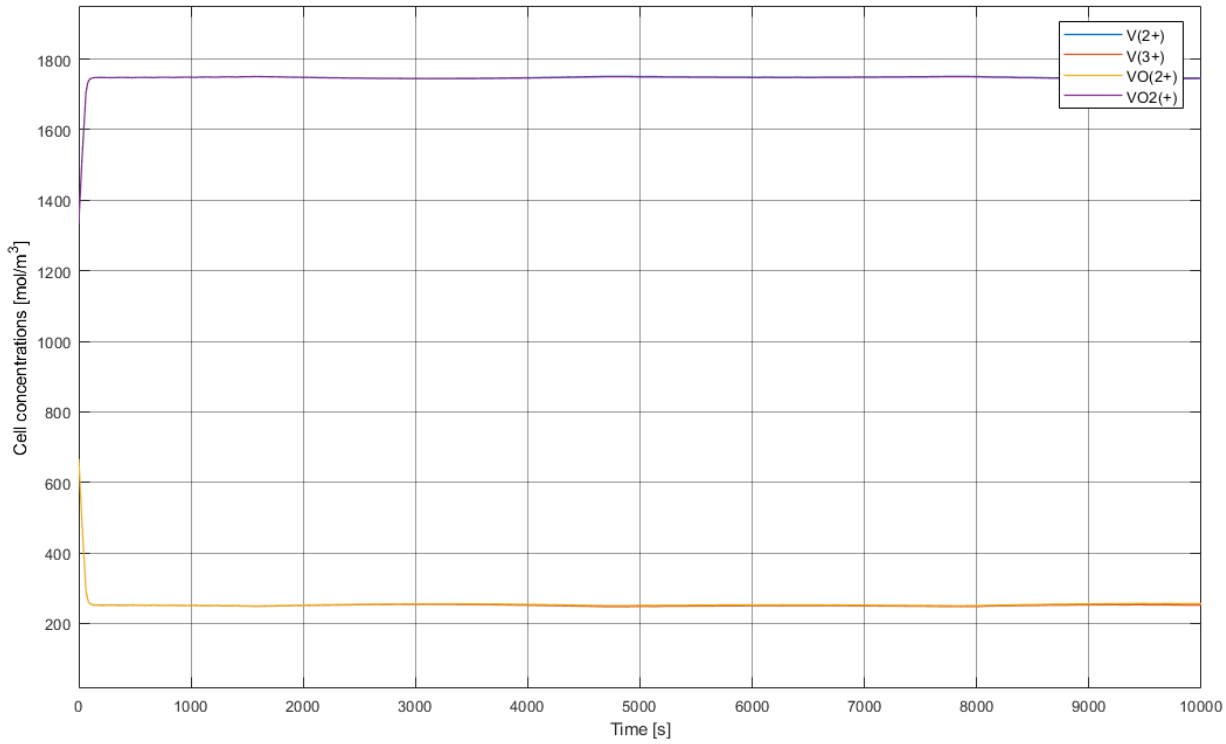

Figure 42. Third simulation's cell concentrations.

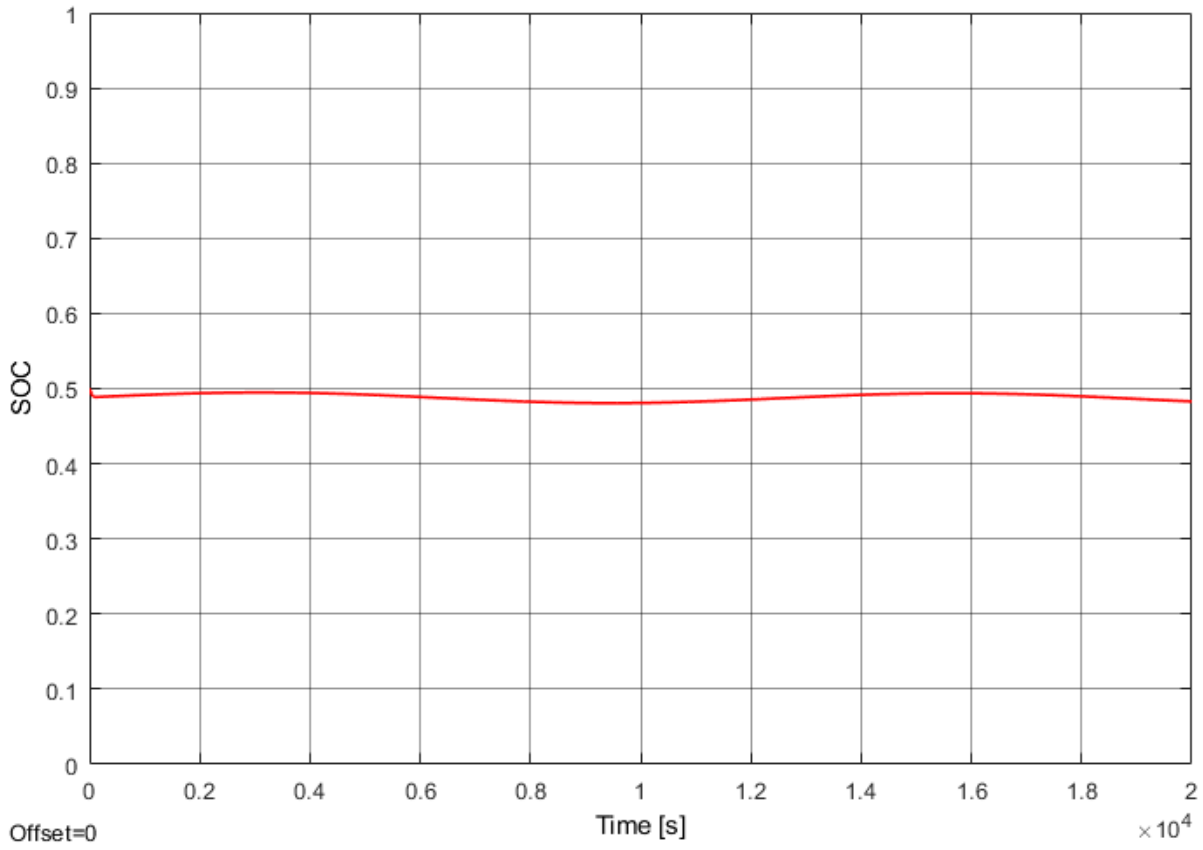

Figure 43. Third simulation's state of charge.

The oscillating input current of Figure 39 is a sinusoidal signal with an amplitude of 100 A, a frequency of 0.001 rad/s and an initial phase of π/2 rad.

The voltages in Figure 40 remain satisfactorily close, reassuring the work of the designed controller. When looked closely, it is appreciable how the output voltage does not follow the reference voltage steadily, as it oscillates a tiny bit at the peaks of the current sinusoid. In the zoomed-in Figure 41, it is observable how the negative current peaks make the voltage oscillate more than the positive ones, the maximum difference between the reference voltage and the output voltage is 0.06, which is an error of only 0.01%.

Figure 42 shows how the cell concentration also oscillate very subtly throughout the simulation, but they stay more or less at a steady value.

The state of charge in Figure 43 also oscillates around the initial 50% value. As with the cell voltage, the biggest oscillations seem to coincide with the negative peaks of the input current.

6. ENVIRONMENTAL IMPACT

The scope of this project is purely theoretical. It attempts to model and simulate the behaviour of a hypothetic system that could be built in real life and, therefore, virtually no resources have been used to develop it.

Of course, redox flow batteries in the real world do have a strong environmental impact. Their purpose is mainly to aid the transition to environmentally friendly energies from non-renewable power. They are already an improvement to current big scale lithium-ion batteries due to their extraordinary long life and the fact that vanadium is quite an innocuous chemical substance, both for humans and for the environment specially when compared to fossil fuels.

One of the main characteristics of VRFBs is that they are quite large when compared to other forms of energy storage. So, in big scale applications, for instance, they could affect landscapes or need several resources for building them; however, the upsides seem far numerous and greater than the downsides when it comes to environmental impact.

All in all, the use of VRFBs could mean a big step forward for the renewable energies takeover and eventually have a positive impact in the planet's wellbeing.

For an estimation of the environmental impact from the development of this project itself: the laptop that has been used needs about 100 W to work; considering about 270 hours of work done on the laptop for the project, the resulting energy consumption comes at around 27 kW·h.

7. BUDGET

In order to calculate the budget, it will be assumed that a student of the bachelor's degree in Industrial Technology Engineering in an internship could earn about 10 €/hour. With that in mind, Table 4 shows a breakdown of the budget for this project.

Table 4. Budget breakdown.

WORKING COST	Hours	Cost
Research	30	150 €
MATLAB programming	70	800 €
System modelling	40	500 €
Simulation and analysis	60	600 €
Writing of the project report	70	700 €
Total working cost	**2750 €**	

EQUIPMENT COST	Cost
MATLAB and Simulink Student Suite	69 €
Microsoft Office for students	79 €
Laptop	1000 €
Total equipment cost	**1148 €**

8. CONCLUSIONS

Redox flow batteries and, in the case of this project, vanadium redox flow batteries are a very promising technology. A lot of work is being put into its research, its implementation and the mitigation of some of its problems, but it seems that it is still a long way away of becoming a standardized energy storage option both in industries and homes.

The modelling of this project has been entirely based on mathematical models that already existed in the body of work of VRFBs, and they seem to yield realistic results in the simulations. The results of this project show how it is possible to develop a control system that automatizes and ensures the correct functioning of a VRFB. The control method did not need to be very sophisticated or innovative as the objective was achieved with a system controlled by a PI controller and a feedback.

It is important to remember the constraints under which the model of the project has been developed, such as the assumption of an unchanging concentration in the battery tanks or the avoidance of either very high or very low states of charge. These assumptions are plausible in big scale applications such as industries that require or generate a lot of power; or homes -like the one imagined in this project- that would need to store large amounts of energy at a time due to the conditions of their environment. However, if a smaller scale application was to be analysed -for instance, a battery that could store a day's worth of energy in a small home-, these factors should probably be taken into consideration.

All in all, redox flow batteries possess unique properties that make them great at aspects that conventional batteries cannot compete with, specially working in large scale applications. With more efforts in the development of the technology and their implementation in real life, RFBs can potentially be the key for a renewable energy-powered future.

9. ACKNOWLEDGEMENTS

I would like to thank Ramon Costa Castelló for teaching me new things about control engineering and knowledge of redox flow batteries; and for his patience, availability and interest shown in the project.

10. BIBLIOGRAPHY

[1] THE INDEPENDENT ICELANDIC AND NORTHERN ENERGY PORTAL. The energy sector. [https://askjaenergy.com/iceland-introduction/iceland-energy-sector, accessed on 14 May 2019]

[2] EMBURY-DENNIS, T. Costa Rica's electricity generated by renewable energy for 300 days in 2017, The Independent, 2017. [https://www.independent.co.uk/news/world/americas/costa-rica-electricity-renewable-energy-300-days-2017-record-wind-hydro-solar-water-a8069111.html, accessed on 14 May 2019]

[3] SWEDISH ENERGY AGENCY. Energy use in Sweden. [https://sweden.se/SOCiety/energy-use-in-sweden, accessed on 14 May 2019]

[4] WINDEUROPE. Wind energy in Europe in 2018. [PDF] [https://windeurope.org/wp-content/uploads/files/about-wind/statistics/WindEurope-Annual-Statistics-2018.pdf, accessed on 14 May 2019]

[5] DEBORD, M. Elon Musk's big announcement: It's called 'Tesla Energy', Business Insider, 2015. [https://www.businessinsider.com/here-comes-teslas-missing-piece-battery-announcement-2015-4?IR=T, accessed on 14 May 2019]

[6] FIELD, K. Everything You Need to Know About the Tesla Powerwall 2 (2019 Edition), 2019 [https://cleantechnica.com/2019/01/19/everything-you-need-to-know-about-the-powerwall-2-2019-edition/, accessed on 20 May 2019]

[7] NELSEN, A. Electric cars emit 50% less greenhouse gas than diesel, study finds, The Guardian, 2017. [https://www.theguardian.com/environment/2017/oct/25/electric-cars-emit-50-less-greenhouse-gas-than-diesel-study-finds, accessed on 14 May 2019]

[8] TESLA TEAM. Introducing V3 Supercharging. [https://www.tesla.com/blog/introducing-v3-supercharging, accessed on 14 May 2019]

[9] INTERNATIONAL ENERGY AGENCY. Clean Energy Ministerial, and Electric Vehicles Initiative (EVI), 2017. "Global EV Outlook 2017: Two million and counting" [PDF] [https://www.iea.org/publications/freepublications/publication/GlobalEVOutlook2017.pdf, accessed on 20 May 2019]

[10] EMBIBE. Redox reaction as electron transfer reaction [JPEG] [https://www.embibe.com/study/redox-reaction-as-electron-transfer-reaction-concept, accessed on 20 May 2019]

[11] WEREWOLF, S. Lithium vs silicon lithium-ion battery scheme, Wikimedia Commons [PNG] [https://commons.wikimedia.org/wiki/File:Lithium_vs_silicon_lithium-ion_battery_scheme.png, accessed on 20 May 2019]

[12] GROLLEAU, S. DELAILLE, A. HAMID, G. Predicting lithium-ion battery degradation for efficient design and management, World Electric Vehicle Journal Vol. 6, 2013.

[13] BELLIS, M. Biography of Alessandro Volta – Stored Electricity and the First Battery, 2017. [https://www.thoughtco.com/alessandro-volta-1992584, accessed on 20 May 2019]

[14] ODULANDE, E. Different Types of batteries and their applications, 2018. [https://circuitdigest.com/article/different-types-of-batteries, accessed on 20 May 2019]

[15] BARTOLOZZI, M. J. Nucl. Sci. Tech. 37, 2000.

[16] ZHAOXIANG, Q. KOENIG, G. M. Review Article: Flow battery systems with solid electroactive materials. Journal of Vacuum Science & Technology B, Nanotechnology and Microelectronics: Materials, Processing, Measurement, and Phenomena, 2017.

[17] AL-FETLAWI, H. Modelling and simulation of all-vanadium redox flow batteries, Ph.D. thesis, University of Southampton, 2010.

[18] WHITE, R.E. WALTON, C.W. BURNEY, H.S. BEAVER, R.N. Journal Electrochem. Soc. 133, 1986

[19] FUJIMOTO, C. KIM, S. STAINS, R. WEI, X. LI, L. YANG, Z. G. Vanadium redox flow battery efficiency and durability studies of sulfonated Diels Alder poly(phenylene)s, Electrochemistry Communications, Volume 20, 2012.

[20] SKYLLAS-KAZACOS, M. KASHERMAN, D. HONG, D. KAZACOS, M. Characteristics and performance of 1 kW UNSW vanadium redox battery, J. Power Sources, 1991.

[21] RITCHIE, I.M. SIIRA, O.T. Redox batteries- an overview, 8th Biennial Congress of the International Solar Energy Society Proceedings, 1983.

[22] KRISTENSEN, S. Picture of the oxidation states of vanadium (2,3,4,5), Wikimedia Commons [PNG] [https://commons.wikimedia.org/wiki/File:Vanadiumoxidationstates.jpg, accessed on 22 May 2019]

[23] XIAO, W. TAN, L. Control strategy optimization of electrolyte flow rate for all vanadium redox flow battery with consideration of pump, Renewable Energy, 2018.

[24] KÖNIG, S. SURIYAH, M.R. LEIBFRIED, T. Model based examination on influence of stack series connection and pipe diameters on efficiency of vanadium redox flow batteries under consideration of shunt currents, Journal of Power Sources, 2015.

[25] ONTIVEROS, L.J. MERCADO, P.E. Modeling of a Vanadium Redox Flow Battery for power system dynamic studies, Elsevier, 2013.

[26] ENERGIA BARCELONA. Calculadora energètica [http://energia.barcelona/ca/calculadora-energetica, accessed on 31 May 2019]

[27] KÖNIG, S. SURIYAH, M.R. LEIBFRIED, T. Innovative model-based flow rate optimization for vanadium redox flow batteries, Journal of Power Sources, 2016.

[28] CUNHA, A. MARTINS, J. RODRIGUES, N. BRITO, F. P. Vanadium Redox Flow Batteries: a Technology Review, International Journal of Energy Research, Elsevier, 2015

[29] GUNDLAPALLI, R. KUMAR, S. JAYANTI, S. Stack Design Considerations for Vanadium Redox Flow Battery, INAE letters, 2018

[30] GAGNIUC, A. P. Markov Chains: From Theory to Implementation and Experimentation, John Wiley & Sons, 2017.

[31] TANG, A. BAO, J. SKYLLAS-KAZACOS, M. Studies on pressure losses and flow rate optimization in vanadium redox flow battery, J. Power Sources, 2014

[32] DE PERSIS, C. Linear versus nonlinear systems and linearization, Control Engineering Lecture 3 ver. 1.4.2, Rijksuniversiteit Groningen, 2018 [PDF]